Unveiling *Leishmania* invasion of fibroblasts: calcium signaling, lysosome recruitment and exocytosis culminate with actin-independent invasion.

Short Title: Leishmania amazonensis hijacks host cell lysosomes to actively induce invasion in fibroblasts.

Victor Soares Cavalcante-Costa[1]; Mariana Costa-Reginaldo[1]; Thamires Queiroz-Oliveira[1]; Anny Carolline Silva Oliveira[2]; Natália Fernanda Couto[2]; Danielle Oliveira dos Anjos[3]; Jane Lima-Santos[3]; Luciana de Oliveira Andrade[2]; Maria Fátima Horta[1] and Thiago Castro-Gomes[1]*.

[1]*Departamento de Bioquímica e Imunologia,* [2]*Departamento de Morfologia, Instituto de Ciências Biológicas, Universidade Federal de Minas Gerais, 31270-901, Minas Gerais, Brasil.*

[3]*Departamento de Ciências Biológicas, Universidade Estadual de Santa Cruz, 45662-900, Bahia, Brasil.*

victor.soaresce@hotmail.com (Victor Soares Cavalcante-Costa); mariana7l00@gmail.com (Mariana Costa-Reginaldo); thamires.olivv@gmail.com (Thamires Queiroz-Oliveira); ninalarrude@gmail.com (Anny Carolline Silva Oliveira); naticouto.92@gmail.com (Natália Fernanda Couto); doanjos@uesc.br (Danielle Oliveira dos Anjos); jlsantos@uesc.br (Jane Lima-Santos); lucianaandrade@ufmg.br (Luciana de Oliveira Andrade); phorta@icb.ufmg.br (Maria Fátima Horta); thiagocg@gmail.com (Thiago Castro-Gomes).

*Corresponding author and present address:
Departamento de Parasitologia, ICB, UFMG
Av. Antônio Carlos, 6627 - Campus Pampulha
Belo Horizonte, MG 31270-901, Brazil
Phone: +55-31-3409-2969
e-mail: Thiago Castro-Gomes : thiagocg@gmail.com

ABSTRACT

Intracellular parasites of the genus *Leishmania* are the causative agents of human leishmaniasis, a widespread emergent tropical disease. The parasite is transmitted by the bite of a hematophagous sandfly vector that inoculates motile flagellated promastigote forms into the dermis of the mammalian host. After inoculation, parasites are ultimately captured by macrophages and multiply as round-shaped amastigote forms. Macrophages seem not to be the first infected cells since parasites were observed invading neutrophils first whose leishmania-containing apoptotic bodies were latter captured by macrophages, thereby becoming infected. The fact that *Leishmania spp* are able to live and replicate inside immune phagocytic cells and that macrophages are the main cell type found infected in chronicity created the perception that *Leishmania spp* are passive players waiting to be captured by phagocytes. However, several groups have described the infection of non-phagocytic cells *in vivo* and *in vitro*. The objective of this work was to study the cellular mechanisms involved in the invasion of non-professional phagocytes by *Leishmania*. We show that promastigotes of *L.amazonensis* actively induces invasion in fibroblasts without cytoskeleton activity, thus by a mechanism that is distinct from phagocytosis. Inside fibroblasts parasites transformed in amastigotes, remained viable for at least two weeks and re-transformed in promastigotes when returned to insect vector conditions. Similarly to what was observed for *T. cruzi*, infection involves calcium signaling, recruitment and exocytosis of lysosomes involved in plasma membrane repair and lysosome-triggered endocytosis. Conditions that alter lysosomal function such as cytochalasin-D and brefeldin-A treatment or the knockout of host cell lysosomal proteins LAMP-1 and 2 dramatically affected invasion. Likewise, triggering of lysosomal exocytosis and lysosome-dependent plasma membrane repair by low doses of streptolysin-O dramatically increased parasite entry. Together our results show that

L.amazonensis promastigotes are able to take advantage of calcium-dependent lysosomal exocytosis and lysosome-induced endocytosis to invade and persist in non-phagocytic cells.

AUTHOR SUMMARY

Intracellular parasites of the genus *Leishmania* are the causative agents of leishmaniasis. The disease is transmitted by the bite of a sand fly vector which inoculates the parasite into the skin of mammalian hosts, including humans. During chronic infection the parasite lives and replicates inside phagocytic cells, notably the macrophages. An interesting but overlooked finding on *Leishmania* infection is that non-phagocytic cells have also been found infected by amastigotes. Nevertheless, the mechanisms by which *Leishmania* invades non-phagocytic cells were not studied to date. Here we show that *L. amazonensis* can actively induce their own entry into fibroblasts independently of actin cytoskeleton activity, thus by a mechanism that is distinct from phagocytosis. Invasion involves subversion of host cell functions such as calcium signaling and recruitment and exocytosis of host cell lysosomes involved in plasma membrane repair and whose positioning and content interfere in invasion. Parasites were able to replicate and remained viable in fibroblasts, suggesting that cell invasion trough the mechanism demonstrated here could serve as a parasite hideout and reservoir, facilitating infection amplification and persistence.

INTRODUCTION

The genus *Leishmania* comprises several species of intracellular parasites that cause a group of diseases collectively known as leishmaniasis. This parasitic infection is typical of tropical countries and occurs in several regions around the globe, affecting around 14 million people and generating 1 million new cases each year [1]. The disease is closely linked to poverty and is associated with malnutrition, population displacement, poor housing, immunosuppression and lack of financial resources. The outcome of the disease depends on the species and strain of the parasite and on the immunological and nutritional status of the patient. The cutaneous form of leishmaniasis is commonly caused by the species *L. braziliensis*, *L. major* and *L. amazonensis*, and is characterized by the formation of skin lesions that can either heal spontaneously over time or evolve to a chronic condition, which can disseminate and lead to massive tissue damage. The most severe form of the disease is known as visceral leishmaniasis, commonly caused by the species *L. donovani* and *L. infantum*, which affects internal organs such as the spleen and liver and is responsible for the majority of fatal cases.

Evolving a way to cross the host plasma membrane (PM) is a mandatory step for intracellular pathogens to establish infection. Therefore, a multitude of strategies to penetrate cells were developed by different microorganisms. Cell invasion can be accomplished through formation of a moving junction that drives parasites into cells as observed with the protozoans *Toxoplasma gondii* and *Plasmodium spp.* [2], direct injection of parasites through a specialized structure that punctures the PM as in microsporidians [3], induction of phagocytosis as in *Leishmania*, *Listeria*, *Chlamydia* and others [4] or subversion of host cell endocytic pathways as in *Trypanosoma cruzi* [5]. In the case of *Leishmania spp*., the parasite is transmitted by the bite of infected female phlebotomine hematophagous sand flies, which inject the flagellated infective promastigote forms into the mammalian host during blood

meals. Once inside the mammalian host, promastigotes are ultimately captured by macrophages, which are considered to be their main host cells and in which parasites replicate as intracellular round-shaped forms, the amastigotes.

It has been reported that, before parasites reach macrophages, promastigotes are phagocytosed by neutrophils, the first immune cells to be recruited to infection site a few minutes after inoculation into the dermis [6]. Inside neutrophils, and already transformed into amastigotes, parasites are able to induce the apoptotic death of the host cell whose leishmania-containing apoptotic bodies are later captured by macrophages, which thereby become infected [7] [8]. Because in the lesions amastigotes are mainly observed inside macrophages, these cells are the most studied and the best established infection model. However, cells unable to perform classical phagocytosis, such as fibroblasts, epithelial and muscle cells, have been reported to harbor *Leishmania spp.* amastigotes *in vitro* and *in vivo* [9] [10] [11] [12]. Despite its potential importance, the mechanism by which *Leishmania spp.* invade such cells remains elusive. Therefore, we sought to investigate how the parasite invades cells unable to perform classical phagocytosis using fibroblasts and *Leishmania amazonensis* promastigotes as a model. Our results have shown that, *in vitro*, much like the related trypanosomatid protozoan *T. cruzi*, *L. amazonensis* subverts host cell endocytic pathways, triggering calcium signaling, lysosome recruitment and exocytosis to induce cell invasion in an actin cytoskeleton-independent fashion.

RESULTS

***L. amazonensis* invades mouse embryonic fibroblasts (MEFs) *in vitro*.** In order to verify whether *L. amazonensis* was able to invade MEFs, the cells were incubated with *LLa*-RFP parasites for 1 h and stained with phalloidin-A488 and DAPI. Cells were analyzed by fluorescence microscopy using Zeiss-Apotome microscope to obtain confocal images. In figure 1A, a 3D reconstruction including all *z* stacks obtained for an infected cell is shown and displays the internalized parasite in the fibroblast (all stacks are provided in supplementary figure S1A). In figure 1B, a single focal plane of the same infected fibroblast shows a parasite (red) not co-localized with host cell F-actin (green), suggesting that invasion does not depend on cytoskeleton activity. Parasites were never observed co-localized with F-actin, which already suggested that cell entry does not need cytoskeleton activity - extra images of infected cells stained for F-actin are provide in Supplementary Figure S2A. To examine the kinetics of infection, we quantified infection rate by flow cytometry. Figure 1C shows that as early as 15 min about 18% of cells were RFP-positive. From 30 min to 4 h there were no substantial changes, but after 24 h, 50% of the cells were infected. Since external parasites can be easily removed by trypsin treatment, we can assume that RFP-positive cells are the infected cells.

To verify whether host cell actin polymerization participates in the process of invasion, MEFs were pre-treated with cytochalasin D to inhibit actin polymerization, and infection was assessed. The result (Fig. 1D) shows not only that host cell actin polymerization is dispensable for cell invasion, but that actin filament disassembly facilitates parasite entry, leading to almost four-fold increase in the infection rate. In order to determine whether invasion of MEFs is a unique property of metacyclic promastigotes, cells were incubated with either procyclic or metacyclic *LLa*-RFP promastigotes (Fig. 1E). We observed that, unlike metacyclic forms, procyclic promastigotes were not able to infect cells, indicating that the ability to invade MEFs

is acquired during metacyclogenesis. To determine whether cell entry depended on the viability of parasites, MEFs were incubated with PFA-fixed or heat-treated *LLa*. We observed that, while the infection rate by living parasites reached 18% (4 h) and 56% (24 h), no PFA-fixed or heat-treated promastigotes were internalized by MEFs, apart from a negligible amount of heat-treated parasites at 24 h (Fig. 1F and G). This result showed that only living metacyclic promastigotes are able to enter MEFs.

In order to determine whether lysosomes fused with parasite-containing intracellular compartments, we stained cells with antibodies against the lysosomal protein LAMP-2 and analyzed cells by fluorescence microscopy. Figure 1H shows a single focal plane of an infected fibroblast harboring a parasite surrounded by LAMP-2 (green) after 2 h of infection, demonstrating that the parasites are fully surrounded by a membrane containing the lysosomal marker LAMP-2. Additional z stacks from this experiment are shown in supplementary figure S1B.

***L. amazonensis* persists and replicates within LAMP-containing vacuoles inside fibroblasts.** In order to evaluate the fate of the parasites internalized in fibroblasts and their ability to replicate within the host cell, we analyzed the infected population by flow cytometry after 4 and 24 h of infection. Our results showed that the RFP mean fluorescence intensity of the infected population doubled at 24 h post infection, indicating that parasites were able to replicate inside fibroblasts (Fig. 2A). To evaluate whether parasites persist inside LAMP-containing vacuoles, we performed an immunofluorescence assay in which cells infected with *LLa*-RFP were fixed, labeled with anti-LAMP-1 antibody and analyzed after 24 h of infection. Figures 2B and C show two intracellular parasites with the typical amastigote morphology inside independent LAMP2-positive vacuoles in the perinuclear region. This result shows that, upon uptake, *L. amazonensis* survives and is able to differentiate from metacyclic promastigotes into replicating amastigotes inside vacuoles with properties of lysosomes,

similar to what occurs in macrophages. Images obtained by transmission electron microscopy confirmed the presence of amastigotes within host cell parasitophorous vacuoles (PV) (Figure 2D, white and black asterisks). These images revealed the characteristic subpellicular microtubules (SM) of *Leishmania* amastigotes and a close juxtaposition between the parasitophorous vacuole membrane (PVM) and parasite membranes (Fig. 2E and insert). After a week of infection amastigotes were still observed inside single PVMs (Fig. 2F), and the parasites showed no detectable alterations in their typical ultrastructural organization, such as nucleus (N), mitochondria (M) and flagellar pocket (FP) (Fig 2G). After 10 days of infection we could still observe cells containing viable amastigotes (Fig 2H and I), as demonstrated by their ability to re-transform into flagellated promastigotes (Fig. 2J) after host cells were scraped off, inoculated into promastigote culture medium and incubated at 24^{o}C for a week.

***In vitro* infection of fibroblasts by *L. amazonensis* involves calcium signaling, plasma membrane permeabilization and lysosome recruitment/exocytosis.** Cell invasion by intracellular parasites often involves calcium signaling, which can induce changes in the PM that promote parasite entry [13] [14] [15] [16] [5]. In order to evaluate whether *L. amazonensis* metacyclic promastigotes trigger calcium signaling in fibroblasts, we loaded MEFs with the Fluo-4AM calcium probe before inoculation of *LLa*-RFP and recorded fluorescence changes during the first 15 min of parasite-host cell contact. Intense intracellular calcium transients were detected in fibroblasts (Fig. 3A and supplementary video 1), from the first minute of incubation and continuing throughout the 15 min recorded. Figure 3B shows quantification over time of the Fluo-4AM fluorescence intensity of each indicated cell, displayed as a graphic representation of the multiple calcium transients induced in MEFs by contact with *L. amazonensis* metacyclic promastigotes. To verify whether calcium was flowing from the extracellular milieu to the cytoplasm through wounds caused by the parasites

on the PM, a monolayer of MEFs was incubated with *L. amazonensis* metacyclic promastigotes in the presence of PI and then analyzed by live fluorescence microscopy. We saw that, in the presence of parasites, some host cells become PI-positive, showing that *L. amazonensis* promastigotes can induce PM permeabilization (Fig. 3C). When PI was added only at the end of the infection period and the cell population was analyzed by flow cytometry, we observed that 18% of the fibroblasts were stained by PI in the absence of calcium (Fig. 3D). On the other hand, no significant PI staining was observed when cells were exposed to the parasites in the presence of calcium (Fig.3D), indicating that PM permeabilization is transient and that cells are able to recover when calcium is present. To evaluate whether the presence of calcium in the extracellular media is important for parasite entry, we performed the infection assay in the presence of increasing concentrations of calcium. The result (Fig.3E) shows that while in low calcium medium the infection is poor, the presence of free calcium in the media favors infection in a dose-dependent manner. Since calcium transients could also be generated intracellularly by second messengers triggered by the contact with parasites, as previously shown for *T. cruzi* and other parasites [17], the same experiment (shown in figure 3A) was performed in calcium-free medium. As observed, parasites were able to trigger calcium signaling even when calcium was absent in the extracellular media (Figs. 3 F and G). Together these results demonstrate that both intracellular calcium signaling and extracellular calcium influx occur during contact of *L. amazonensis* promastigotes and host fibroblasts.

One of the consequences of calcium rising in the cytosol is the triggering of lysosomal exocytosis, an important step during the process of PM repair [18]. In the latter, the exocytosis of lysosomes triggers the internalization of the wounded membrane by endocytosis [19], a process that may be subverted by endoparasites to invade cells [5]. To assess whether host cell lysosomes were recruited to parasite binding site, we incubated MEFs with *L. amazonensis*, and permeabilized and labelled the cells to visualize lysosomes. The result (Fig.

4A) shows that host cell lysosomes are attracted and polarized towards parasite attachment site. To verify whether lysosomes were also exocytosing their content upon contact *L. amazonensis*, MEFs were incubated with *LLa*-RFP and then labeled with anti-LAMP-1 antibodies, this time without cell permeabilization. We observed that cells exposed luminal lysosomal protein epitopes on the extracellular leaflet of the PM (Fig.4B), indicative of lysosomal exocytosis. Quantification by flow cytometry (Fig. 4C) shows that around 30% of cells incubated with live parasites exposed LAMP-1 on their surface, an event not triggered by fixed parasites. Lysosomal exocytosis during cell entry was further confirmed by detecting beta-Hexosaminidase enzymatic activity (Fig. 4D) and the presence of acid sphingomyelinase (ASM) and cathepsin-D (Fig. 4E) in culture supernatants during host cell exposure to living *L. amazonensis* promastigotes. In order to verify whether contact with parasites also enhanced endocytosis levels in MEFs, cells were labeled with WGA-Alexa-488 to stain the plasma membrane and incubated with parasites for 15 min. After quenching the remaining extracellular fluorescence with trypan blue, the endocytosed dye was quantified by flow cytometry. The result (Fig. 4F) shows that the presence of parasites increases endocytosis in MEFs, thus making cells more susceptible to invasion.

Since exocytosis of lysosomes is followed by a massive endocytosis [20] and generates ceramide-rich vacuoles [5] in an actin polymerization-independent manner, we decided to evaluate the presence of lysosomal markers and ceramide in vacuoles of recently internalized parasites. Cells were then infected with *LLa*-RFP for 1h and labeled with anti-LAMP1 or anti-ceramide antibodies. As anticipated, parasites were completely surrounded by lysosomal markers and ceramide and both perfectly delineated bodies and flagella of the internalyzed metacyclic promastigotes (Fig. 4G and H). Conversely, and as previously stated, newly formed parasitophorous vacuoles were never covered by F-actin filaments (Fig. 1B and

Supplementary Figure S2A). Together, these results indicated that the invasion process involves early lysosomal fusion and exocytosis, as previously demonstrated for *T. cruzi* [21].

Invasion of fibroblasts by *L. amazonensis* involves the recruitment of lysosomes to the infection site to form the nascent parasitophorous vacuole. In order to follow the recruitment of lysosomes to the parasite entry site, we carried out a time-course infection of MEFs by *LLa*-RFP, and prepared cells for fluorescence microscopy using anti-LAMP-1 antibodies. At 15 min of infection, we started to observe parasites closely interacting with fibroblasts and presenting an intense co-localization with LAMP-1 at the flagellar portion (Fig. 5A). This contact with infective promastigotes creates a lysosomal polarization towards parasite binding site at the very beginning of invasion process (Fig. 4A, Fig. 5A and Supplementary Figure S2B). At 30-60 min of interaction, parasites are often observed with the flagella completely internalized and co-localized with lysosomal proteins whilst parasite body remains partially unlabeled (Figs. 5B) and surrounded by a LAMP-1-positive pocket. At 90 min, we observed parasites totally internalized, completely covered by the lysosomal marker and already located at the perinuclear region. At this point, we also started to observe the shortening of the flagella (Fig 5C). From 120 min (Fig. 5D) to 24 h (Fig. 5E), parasites were found close to the nuclei inside a juxtaposed oval- or round-shaped vacuole, completely surrounded by the lysosomal protein and with no detectable flagella, in a typical amastigote morphology.

Lysosomal positioning and undamaged lysosomes are essential for fibroblast invasion by *L. amazonensis*. Lysosomes can be pre-linked to the PM at the cell periphery [22] [23] and associated with microtubules [24]. In order to evaluate the role of microtubule-based movement of lysosomes in fibroblast invasion by *L. amazonensis*, we treated cells with the microtubule-blocking agent nocodazole before infection. There was no difference in invasion between cells treated or not with nocodazole (Fig. 6A), suggesting that PM-

associated lysosomes might be sufficient to induce invasion. Cytochalasin D and brefeldin-A are drugs known to lead to lysosome accumulation at cell periphery [21]. MEFs previously treated with each of these drugs showed a massive increase in infection (Figs. 6B and C). However, this increase was markedly blocked by nocodazole treatment (Figs. 6B and C). Cytochalasin D and brefeldin-A treatment not only led to an increase in infected cells but also to a higher number of parasites per cell, as we could observe by fluorescence microscopy (Fig. 6D, 6E and 6F) and measure by flow cytometry, which showed about 2-fold increase in mean fluorescence intensity (not shown).

Lysosomes are essential organelles whose exocytosis promotes the removal of PM lesions by endocytosis. To better evaluate the role of lysosomes in cell infection and specifically address whether PM repair is important for cell invasion, we performed the infection of LAMP-2 knockout and LAMP-1/2 double knockout MEFs with *LLa*-RFP. These cells are known to be deficient in PM repair due to the accumulation of cholesterol and caveolin in lysosomes and, for this reason, are less susceptible to the invasion of *T. cruzi* [25]. The results (Fig. 6G to I) show that the absence of these lysosomal proteins dramatically impairs *L. amazonensis* invasion.

Generation of transient PM wounds during parasite-host cell interaction increases invasion. Lysosome recruitment to cell periphery and lysosomal exocytosis are events that can be triggered by transient PM disruption. Calcium influx through SLO pores, for example, leads to calcium-dependent exocytosis of lysosomes, which is followed by a massive compensatory endocytosis that removes the damaged membrane from cell surface [19]. Since we observed that parasites were inducing all these processes during cell entry, we decided to test whether inducing additional PM permeabilization during invasion would result in higher infection rates. First we established an ideal concentration of SLO to obtain the maximum PM damage (in the absence of calcium) with total cell recovery (in the presence of

303 calcium) (Fig. 7A). Cells started to become permeabilized (PI-positive) at 50 ng/ml SLO, a
304 concentration in which almost 100% of the cells were able to repair their PM (PI-negative)
305 (blue curves). When MEFs were treated with repairable concentrations of SLO during a 15
306 min of incubation with *L. amazonensis*, infection of the cell population not only doubled (Fig
307 7B) but the number of parasites/cell also increased, as observed by around a 2-fold increase
308 in the mean fluorescence intensity of each infected cell for both treatments (not shown). The
309 massive increase in invasion provoked by SLO-treatment was also visualized when anti-
310 LAMP-1-labeled infected cells were analyzed by fluorescence microscopy (Fig 7C to E). The
311 results showed multi-infected cells (Fig 7D) in which parasites also subsequently transformed
312 into the replicating amastigote forms (Fig. 7E).

313 **DISCUSSION**

314 The remarkable ability of *Leishmania spp.* to survive and replicate inside phagocytes,
315 such as neutrophils, macrophages and dendritic cells, has captured most of the attention and
316 driven nearly all research in this field during the last decades. However, these parasites are
317 also able to infect and survive in non-phagocytic cells, a feature already observed by several
318 authors *in vitro* and *in vivo* [9] [11] [12] [26] (reviewed by Rittig & Bogdan, 2000). In spite
319 of the importance of such observations, almost no effort has been made to understand how
320 these parasites succeed in infecting cells that are unable to perform classical phagocytosis.
321 Here, using MEFs as a model, we show that entry of *L. amazonensis* into fibroblasts is a
322 process that involves the ability of these parasites to actively induce a cell invasion mechanism
323 involving transient PM permeabilization, calcium signaling, lysosome recruitment/exocytosis
324 and lysosome-triggered endocytosis, much like it has been established for another
325 trypanosomatid, *T. cruzi* [28] [21] [5]. Importantly, we demonstrated that this novel invasion
326 mechanism by *L. amazonensis* is not a form of induced phagocytosis, since it does not seem
327 to involve the host cell actin cytoskeleton.

While establishing assays for examining infection of MEFs by *L. amazonensis* promastigotes (Figs. 1A, 1B and 1C), it became evident that these cells could be invaded by the parasites, and that these parasites were found inside lysosome-derived vacuoles (Fig. 1H) as observed for macrophages. However, unlike the phagocytosis-mediated entry that occurs in macrophages, the invasion of MEFs by *L. amazonensis* depends on parasite direct activity, since PFA-fixed promastigotes and heat-treated parasites were not internalized (Figs. 1F and 1G). The conditions inside MEFs parasitophorous vacuoles not only allowed the typical differentiation of promastigotes into amastigotes and their replication (Fig. 2A to C), but also the persistence of viable parasites (Fig. 2H, 2I and 2J), similar to what had been described for *L. donovani* in human fibroblasts [12].

Invasion of several intracellular microorganisms such as *SalmoneLLa typhimurium* [13], group B streptococci [14], *Listeria monocytogenes* [15] and *T. cruzi* [16] [5] is accompanied by, or dependent on, a rapid increase in the levels of free intracellular calcium. In the model described here, contact with live *L. amazonensis* promastigotes also induced strong intracellular calcium transients in MEFs (Fig. 3A-B and 3F-G). Calcium seems to be an important requirement for cell invasion, since its increase in the extracellular medium positively modulated parasite entry (Fig. 3D).

We reasoned that one mechanism for the parasites to trigger calcium elevation in the cytoplasm might be the generation of host cell PM wounds during invasion. Indeed, we showed that contact with live *L. amazonensis* promastigotes wounds the PM of host cells, and the lesions are promptly repaired in the presence of calcium (Fig. 3C and 3D). In fact, when wounded, either by mechanical action or by pore-forming cytolysins, nucleated cells are able to reseal the PM in a process that involves calcium-dependent exocytosis of lysosomes [18]. Extracellularly-secreted lysosomal enzymes were proposed to act on the extracellular leaflet of the PM, triggering the removal of the wounded membrane by endocytosis [19] [29].

353 Calcium-dependent exocytosis of lysosomes is followed by a wave of non-conventional
354 endocytosis [20], which is used by parasites to invade non-phagocytic cells, as previously
355 shown for *T. cruzi* [5]. Thus, we hypothesized that host cell lysosomes are also essential for
356 the infection of fibroblasts by *L. amazonensis*. Indeed, during infection of MEFs with *L.*
357 *amazonensis*, lysosomes were recruited (Fig. 4A, Fig. 5A and Supplementary Figure 2B- 15
358 and 30 min), fused with host cell PM (Fig. 4B-C) and exocytosed their content in the
359 extracellular milieu (Fig. 4D-E). The exocytosis of lysosomes triggered by the parasites was
360 followed by an increase in endocytosis levels in MEFs, indicating that the presence of
361 parasites induces cell responses that facilitate invasion (Fig. 4F). Interestingly, recruitment of
362 lysosomes to the infection site was observed since the very beginning of *L. amazonensis*
363 interaction with MEFs (Fig. 4A, Fig. 5A and Supplementary Figure 2B- 15 and 30 min).
364 Notably, host cell PM wounding and exocytosis of lysosomes had already been observed even
365 in macrophages during *Leishmania* uptake by classical phagocytosis [30], indicating that the
366 mechanism described here might also be important during the invasion of phagocytes.
367 However, in the case of macrophages, it was proposed that lysosomal fusion would be
368 important to reseal PM wounds provoked by the movement of parasites after their
369 internalization [30]. In the case presented here, exocytosis of lysosomes is an event triggered
370 at early steps of parasite-host cell interaction and culminates with parasite internalization.
371 Interestingly, in the experiments described here the exocytosis of the lysosomal enzyme beta-
372 Hex peaked at 15 min of infection (Fig. 4D), matching the early triggering of calcium
373 transients (Fig. 3A) and the appearance of infected cells as early as 15 min after parasite
374 inoculation (Fig. 1C). It is known that after exocytosis from lysosomes, ASM cleaves
375 sphingomyelin on cell surface producing ceramide, a lipid that promotes negative curvature
376 of the PM enabling endocytosis [19]. A ceramide-rich vacuole, as opposed to actin-rich
377 vacuole, is precisely what is observed in endosomes derived from the extracellular action of

ASM during *T. cruzi* internalization [5]. Also similar to earlier observations, we found that recently internalized *Leishmania* parasites are surrounded by a tight PV (Fig. 2E-insert), which is intensely stained by anti-LAMP-1 (Fig. 4G) and anti-ceramide antibodies (Fig. 4H). This indicates that invasion actually takes advantage of exocytosis of lysosomes, which provide the membrane that allows parasite entry, in a mechanism that is markedly distinct from classical parasite internalization by phagocytosis in macrophages. This is corroborated by the facts that *L. amazonensis* parasites can still invade MEFs pre-treated with cytochalasin-D (Fig 1D), and that recently internalized parasites do not co-localize with actin filaments (Fig. 1B and Supplementary Figure S2A). The involvement of lysosomes in the model of invasion described here was further confirmed by the fact that cytochalasin-D and brefeldin-A, two drugs that increase infection rates for *T. cruzi* by boosting the number of peripheral lysosomes, also increased the frequency of *L. amazonensis* infection in MEFs (Fig. 6B and 6C) and the number of parasites per cell, when compared to regular infection conditions (Fig. 6E and 6F). Since both effects could be prevented by nocodazole, a drug that destabilizes microtubules and stops lysosome traffic to cell periphery [24], we can infer that microtubule-associated lysosomes may play a role in infection. Interestingly, nocodazole could not prevent infection by itself, as observed for *T. cruzi* invasion [21], which is probably due to the fact that mammalian cells already have a portion of their lysosomes pre-bound to the PM, which could be sufficient to allow parasite invasion [23]. Moreover, LAMP-2 and LAMP-1/2 knockout cells, which have modified lysosomes and impaired PM repair ability [25] were less susceptible to infection by *L. amazonensis* (Fig. 6H and 6I) when compared to wild type cells (Fig. 6G), similar to what was observed for *T. cruzi* infection with the same cell lines [25]. Additionally, our results indicate that *Leishmania* promastigotes are able to trigger calcium signaling in host cells from intracellular stores (Fig. 3F and G) since signaling also occurs in the absence of extracellular calcium. Further investigation will be needed to identify the

403 molecules involved in this signaling. However, regardless of the origin of the calcium, from
404 extracellular influx or intracellular reservoirs, the downstream effects important for cell
405 invasion such as lysosomal exocytosis and its derived endocytosis would be triggered.

406 We still do not know how parasites induce PM injury in MEFs (Fig. 3C-D). However,
407 at least two possibilities can be raised: 1- parasite movement against the host cell PM could
408 generate mechanical wounds, as previously proposed for *T. cruzi* [5] and 2- the parasites might
409 secrete cytolytic molecules leading to PM permeabilization, as proposed for *Listeria*
410 *monocytogenes* [15]. Since we have described that *Leishmania spp.* produce and secrete pore-
411 forming cytolysins [31] [32] it is possible that these molecules are responsible for
412 permeabilizing host cells during invasion. Both possibilities would trigger calcium influx,
413 induce lysosome exocytosis and trigger endocytosis, playing a key role in promoting parasite
414 invasion. Indeed, when additional PM wounding was induced in MEFs by adding the pore-
415 forming protein SLO during *L. amazonensis* invasion, the frequency of infected MEFs
416 doubled (Fig. 7A and 7B) and multi-infected cells appeared (Fig. 7D). When wounded by
417 SLO at the concentrations used (Fig. 7A) the host cells were able to reseal their PM, allowing
418 the intracellular development of amastigote forms (Fig.7E).

419 Although several authors have already reported the presence of *Leishmania spp.*
420 amastigotes inside non-phagocytic cells *in vivo*, it is well established that, in chronic
421 leishmaniasis, macrophages are the main cell type found parasitized. However, it has already
422 been shown that macrophages may not be the primary cells infected at the bite site, as
423 neutrophils [6] and dendritic cells [33] are found to be infected by promastigotes. This
424 demonstrates that other cells may also be important to sustain the *Leishmania* life cycle. Given
425 that the dermis, where parasites are inoculated, is rich in non-phagocytic cells such as
426 adipocytes, striated muscle cells, epithelial cells and fibroblasts, it is tempting to speculate

that promastigotes may actively induce invasion of these cells *in vivo* through the mechanism described here.

Fibroblasts are actually interesting cells to consider during *in vivo Leishmania* infection, since they are the most abundant cells at the bite site, are major producers of chemokines that attract neutrophils and macrophages, directly interact with macrophages during wound healing and have the ability to move and spread through diapedesis [34] [35]. In addition to the ability of *Leishmania* parasites to induce cell wounding and trigger endocytic repair responses, the phlebotomine vector bite site is known to be an area of intense tissue damage, largely caused by the vector proboscis that damages the surrounding tissue to increase blood supply. Thus, at the bite site, *Leishmania* parasites probably encounter several cell types that are undergoing PM repair, a process known to involve calcium influx, lysosomal exocytosis, actin cytoskeleton rearrangements and endocytosis of wounded membranes. Besides providing a safe location to evade innate immunity, the rapid invasion of non-phagocytic cells shortly after inoculation would allow for a prompt transformation into amastigote forms, which could be later transferred to macrophages or serve as parasite reservoir. The invasion process of new macrophages during chronic infection is not yet fully understood. Amastigotes have been found to be transferred from infected to non-infected cells without cell rupture, either by phagocytosis of infected apoptotic bodies [6] or by direct cell-to-cell transfer of parasites [36]. In this context, further investigation is necessary to define whether active invasion of non-phagocytic cells is an exclusive feature of *Leishmania* promastigotes, or whether amastigotes are also able to do it. Transfer of amastigotes from an infected neutrophil to macrophages, known as the Trojan Horse strategy, was proposed to be a major mechanism allowing *in vivo* invasion of macrophages by *Leishmania spp.* [7]. In this context, it is possible that not only one, but several cell types could be Trojan Horses in *Leishmania spp*. infection, notably at the early stages. Since these parasites are able to

452 replicate inside fibroblasts, as we report here (Fig 2A) and as described by others (reviewed
453 by Rittig and Bogdan, 2000), it is possible that a first round of replication inside these cells
454 could be an important step leading to infection amplification, prior to macrophage invasion.

455 The ability to actively induce cell invasion characterized here is a neglected feature of
456 *Leishmania spp*, probably due to the fact that these parasites have been largely perceived as
457 passive players taken up by phagocytosis. *In vivo* experiments depicting the very first
458 moments of natural infection are difficult to perform and have focused mainly on neutrophils
459 and macrophages, not covering all cell types present at the infection site. Our findings
460 emphasize the importance of performing more accurate and strictly controlled future
461 investigations for characterizing all cell types harboring intracellular *Leishmania* during the
462 first moments of natural infections.

463 **MATERIALS AND METHODS**

464 **1- Parasites and host cells.**

465 The PH8 (IFLA/BR/1967/PH8) strain of *Leishmania (Leishmania) amazonensis* (*LLa*)
466 used throughout this work was provided by Dr. Maria Norma Melo (Departamento de
467 Parasitologia, Universidade Federal de Minas Gerais, Belo Horizonte, Brazil). Parasites were
468 grown at 24^{o}C in Schneider's drosophila medium (Sigma) containing 10% heat-inactivated
469 (hi) fetal bovine serum (FBS) (GIBCO), 100 U/ml penicillin and 100 μg/ml streptomycin
470 (GIBCO). *L. amazonensis* expressing Red Fluorescent Protein (*LLa*-RFP) were kindly
471 provided by Dr. David Sacks (NIH, Bethesda, USA) and cultured as described by Carneiro et
472 al., 2018. *LLa-RFP* promastigotes were grown as described for wild type (WT) promastigotes
473 with further addition of 50 μg/ml of geneticin G418 (Life Technologies), for selection of RFP-
474 expressing parasites. Parasites were cultured for 4-6 days, a period in which cultures become
475 enriched in infective metacyclic promastigotes. Metacyclic forms used in experiments were

476 separated from procyclic forms using a Ficoll gradient, as described by Späth & Beverley,
477 2001.

478 Mouse embryonic fibroblasts (MEFs), WT, LAMP-2 knockout and LAMP-1/2 double
479 knockout cell lines were obtained from from Dr. Paul Saftig's laboratory (Biochemisches
480 Institut/Christian-Albrechts-Universitat Kiel, Germany). Cells were cultured in DMEM
481 (Gibco) containing 10% hi FBS (GIBCO) at 37ºC and 5% CO_2 atmosphere. Cultures were
482 passaged every 48 h and plated, 24 h before experiments, on culture dishes (Sarstedt) or
483 directly on glass coverslips, depending on the experiment. Sub-confluent cultures were used
484 for infection experiments and were analyzed either by fluorescence microscopy or by flow
485 cytometry. In the experiments described here we used 6 well dishes (Kasvi) and plated cells
486 24 h prior to experiment at 3 x 10^5 cells per well. For immunofluorescences round coverslips
487 were placed on the well before cell platting.

488 **2- Infection experiments.**

489 Purified *LLa* metacyclic promastigotes were used throughout the experiments, unless
490 otherwise stated. Parasites were added to dish-adherent MEFs in DMEM containing 10% hi
491 FBS (GIBCO) which were centrifuged at 500 x *g* for 10 min at 15ºC to synchronize parasite
492 contact with cell monolayers, followed by incubation at 37ºC in a 5% CO_2 atmosphere for the
493 indicated periods of time. All experiments were performed using a multiplicity of infection of
494 25 parasites per MEF. For some experiments, parasites were previously fixed in 4% PFA for
495 15 min, or heat-inactivated for 30 min at 56ºC.

496 **3- Cell labeling and western blotting.**

497 ***Immunofluorescence and fluorescent probes*** – MEF sub-confluent monolayers were
498 infected with *LLa*-RFP for the indicated periods of time and fixed with 4% paraformaldehyde.
499 Preparations were blocked/permeabilized with PBS 2% BSA 0.5% saponin and incubated
500 with any of the following antibodies or compounds: rat anti-LAMP-1 IgG (1D4B), rat anti-

LAMP-2 IgG (ABL-93) (obtained from Developmental Studies Hybridoma Bank), mouse anti-ceramide IgM (C8104-50TST) (Sigma) or alexa-488-conjugated phalloidin (Life Technologies). After washing, where appropriate, preparations were incubated for 30 min with alexa-488-conjugated equivalent secondary antibodies (Life Technologies). All preparations were stained with DAPI to visualize nuclei. Coverslips were mounted on microscope slides using anti-fading Prolong-Gold (Life Technologies) and analyzed by fluorescence microscopy. Images were acquired and analyzed using Q-Capture software or Zen Software (ZEISS), depending on the experiment, as indicated. In order to evaluate the exposure of lysosomal epitopes on the PM by flow cytometry (FACS), cells were labeled as described above but without permeabilization in order to detect only extracellular epitopes. For this purpose cells were removed from the dish with a cell scraper before analysis by FACS as described below. ***Western blotting*** - Samples were prepared with reducing sample buffer, boiled for 5 min and fractionated by SDS-PAGE on 10% acrylamide gels (BioRad). After SDS-PAGE, proteins were transferred to a nitrocellulose membrane using a wet transferring apparatus (BioRad). The membrane was blocked with 5% dry milk, followed by overnight incubation with 1:500 rabbit anti-acid sphingomyelinase (ASM) IgG (Abcam cat. # ab83354) or goat anti-cathepsin-D IgG (Santa Cruz sc-6486). After washing, membranes were incubated with the equivalent secondary antibody conjugated with horseradish peroxidase (HRP) (BioRad) at 1:10.000 in 5% dry milk for 1 h. After washing, the membrane was treated with Luminata HRP substrate (Milipore) and analyzed using a LAS-3000 imaging system (Fuji).

3- Quantification and visualization of infection.

FACS - To quantify the rate of infections we took advantage of the *LLa*-RFP described above. After infection experiments, cells were washed, treated with 0.25% trypsin (Gibco) to detach cells and non-internalized parasites and then immediately analyzed the cell population

by flow cytometry using a FACSCAN II (Becton Dickinson). All analyses took into account 10.000 events (MEFs) and were performed using Flow-Jo Software. ***Light Microscopy*** - Visualization of infected cells was performed using BX60 Upright Compound Fluorescence Microscope (Olympus) after staining with a hematoxylin-eosin panoptic stain kit (RenyLab) and mounting on microscopy slides with Entellan (Merk). Images were obtained using Q-CapturePro Software. ***Fluorescence Micros*****copy** – Cells labeled with fluorophore-conjugated antibodies or probes were analyzed with BX60 Upright Compound Fluorescence Microscope (Olympus) or Axio Imager ApoTome2 Microscope (Zeiss) to obtain confocal images. In order to acquire single optical sections, *z* stacks were obtained in the ApoTome mode using structured illumination microscopy technology (SIM). ***Trasmission Electron Microscopy*** - MEFs infected with *L. amazonensis* promastigotes were fixed in 2.5% glutaraldehyde (Sigma), 0.1 M sodium cacodylate buffer (pH 7.2) for 1 h at room temperature. Cells were then washed with 0.1 M sodium cacodylate buffer, collected with a scraper and post-fixed with a solution of 1% osmium tetroxide (O_sO_4) (Sigma), 0.8% potassium ferricyanide and 2.5 mM calcium chloride ($CaCl_2$) for 1 h. After this second fixation step cells were washed and dehydrated in a series ascending concentration of acetone (30-100%). Finally, cells were embedded in PolyBed resin at a ratio of 1:1 (acetone/resin) for 12 h, pure resin for 14 h, and polymerized for 72 h at 60°C. Thin sections were obtained with diamond knives in an ultra-microtome (Leica UC7), collected in copper grids and stained in aqueous solutions of 6% uranyl acetate and 2% lead citrate for 30 and 5 min, respectively. Samples were observed with a Tecnai G2-20-SuperTwin FEI-200 kV Transmission Electron Microscope.

4- Evaluation of PM wounding and repair.

The occurrence of PM wounding was evaluated by determining the degree of exclusion of the impermeant dye propidium iodide (PI), added to cell cultures at 50 μg/mL. PI-treated cells were analyzed by both fluorescence microscopy (EVOS) and flow cytometry. For

fluorescence microscopy experiments using PI, MEFs were plated on 6-well culture dishes and incubated with parasites in HBBS with or without calcium in the presence of PI. To quantify PM wounding by flow cytometry PI was added as indicated, cells were detached from plates with trypsin and analyzed by FACS.

5- Calcium-signaling experiments

MEFs ($1x10^5$ cells per well) were platted in 4-chamber glass bottom dishes and loaded with the calcium probe Fluo 4 (Invitrogen) according to Luo et al., 2011, with slight modifications. Briefly, cells were washed twice with DMEM without FBS and incubated for 50 min with Fluo 4-AM loading solution (Invitrogen). Cells were then washed once with DMEM, 3 times with calcium-free HBSS and maintained in HBSS containing or not 2 mM $CaCl_2$. Calcium transients were recorded by confocal video microscopy (Nikon C2) at 10 frames per second. At 40s of imaging, 5 mM ionomycin (positive control), *LLa*-RFP or HBSS (negative control) were added to the media and the videos were recorded for up to 15 min. Image analysis and quantification of fluorescence were performed using Image-J and NIS Elements (Nikon) software.

5- Detection of lysosomal enzymes.

MEF monolayers were incubated with *LLa* in RPMI without phenol red and supernatants were analyzed for activity of the lysosomal enzyme beta-Hexosaminidase. At the indicated time points, supernatants were collected, centrifuged to remove detached cells and beta-Hexosaminidase activity was determined as described by Rodríguez et al., 1997. Briefly, 100 µl of each supernatant were incubated with 100 µl of 2 mM substrate 4-methyl-umbellyferyl-N-acetyl-b-d-glucosaminide (SIGMA) in 6 mM citrate-phosphate buffer pH 4.5 for 15 min at 37°C. The reaction was stopped with 25 µl of 2 M Na_2CO_3, 1.1 mM glycine and supernatants were read in a fluorimeter at excitation/emission wavelengths of 365/450 nm,

575 respectively. ASM and cathepsin D were detected by western blotting using anti-ASM or anti-
576 cathepsin D antibodies, respectively, under reducing conditions and with samples prepared
577 from FBS-free supernatants after 20 times concentration in a 10 kDa cutoff Amicon®
578 Centrifugal ultra-filter unit.

579 **6- Endocytosis assay**

580 In order to evaluate endocytosis triggered in MEFs by contact with *L. amazonensis*,
581 $3x10^5$ MEFs were plated in a 6-well dish and the outer leaflet of the PM was labeled with 1
582 μg/ml Alexa Fluor 488-conjugated wheat germ agglutinin (WGA) (Life Technologies) for 1
583 min at 4°C. Cells were then exposed or not to *L. amazonensis* promastigotes at 37ºC for 15
584 min followed by treatment with 0.2% trypan blue (Sigma-Aldrich) for 2 min to quench the
585 extracellular fluorescence. After washing, the cell population was removed from the dish by
586 trypsin treatment and analyzed by FACS to detect the remaining cell-associated fluorescence
587 corresponding to the endocytosed dye.

588 **6- Streptolysin-O (SLO) and Drug Treatments**

589 MEF monolayers were treated with 25, 50 or 100 ng/mL of the pore-forming protein
590 streptolysin O (SLO) during infection, or 10 μM cytochalasin-D (SIGMA) for 15 min, or 10
591 μM brefeldin-A for 30 min, or 20 μM nocodazole for 15 min (SIGMA). All drugs were added
592 before infection and were removed from cells after incubation so as to not interfere with
593 parasites viability. To evaluate plasma membrane repair triggered by SLO, fibroblasts were
594 incubated with the indicated concentration of SLO in the absence of calcium (non-repair
595 condition) or after restoring calcium with 2mM $CaCl_2$ (repair condition) – after the addition
596 of propidium iodide cells were analyzed by FACS.

597

598 **7- Repeats**

599 Each experiment in this manuscript was performed in triplicates and the results shown
600 are representative of at least three biological replicates.

601 **ACKNOWLEDGMENTS AND FINANCIAL SUPPORT**

641 We would like to thank Dr. Norma Andrews for reagent donation, advice and critical reading
642 of this manuscript, Dr. Maria Norma Mello for proofreading this manuscript, Dr. David Sacks
643 for kindly providing RFP-expressing parasites, Dr. Paul Saftig for kindly providing cell lines,
644 Elimar Faria for technical support, Jacob Kames and Rodrigo Silva Reston for professional
645 English proofreading and manuscript editing. We also would like to thank CAPI (Centro de
646 Aquisição e Processamento de Imagens) for all support with imaging and microscopy and the
647 Flow Cytometry Laboratory-ICB-UFMG for support with all FACS analysis.

648 **REFERENCES**

649 1. WHO | Leishmaniasis. WHO. World Health Organization; 2018; Available:
650 http://www.who.int/mediacentre/factsheets/fs375/en/

651 2. Besteiro S, Dubremetz J-F, Lebrun M. The moving junction of apicomplexan
652 parasites: a key structure for invasion. Cell Microbiol. 2011;13: 797–805.
653 doi:10.1111/j.1462-5822.2011.01597.x

654 3. Xu Y, Weiss LM. The microsporidian polar tube: A highly specialised invasion
655 organelle. Int J Parasitol. 2005;35: 941–953. doi:10.1016/j.ijpara.2005.04.003

656 4. Schille S, Crauwels P, Bohn R, Bagola K, Walther P, van Zandbergen G. LC3-
657 associated phagocytosis in microbial pathogenesis. Int J Med Microbiol. Urban &
658 Fischer; 2018;308: 228–236. doi:10.1016/J.IJMM.2017.10.014

659 5. Fernandes MC, Cortez M, Flannery AR, Tam C, Mortara RA, Andrews NW.

Trypanosoma cruzi subverts the sphingomyelinase-mediated plasma membrane repair pathway for cell invasion. J Exp Med. 2011;208: 909–921. doi:10.1084/jem.20102518

6. Peters NC, Egen JG, Secundino N, Debrabant A, Kimblin N, Kamhawi S, et al. In Vivo Imaging Reveals an Essential Role for Neutrophils in Leishmaniasis Transmitted by Sand Flies. Science (80-). 2008;321: 970–974. doi:10.1126/science.1159194

7. Laskay T, van Zandbergen G, Solbach W. Neutrophil granulocytes – Trojan horses for Leishmania major and other intracellular microbes? Trends Microbiol. Elsevier Current Trends; 2003;11: 210–214. doi:10.1016/S0966-842X(03)00075-1

8. van Zandbergen G, Solbach W, Laskay T. Apoptosis driven infection. Autoimmunity. 2007;40: 349–52. doi:10.1080/08916930701356960

9. Bogdan C, Donhauser N, Döring R, Röllinghoff M, Diefenbach A, Rittig MG. Fibroblasts as host cells in latent leishmaniosis. J Exp Med. 2000;191: 2121–30. Available: http://www.ncbi.nlm.nih.gov/pubmed/10859337

10. Minero MA, Chinchilla M, Guerrero OM, Castro A. [Infection of skin fibroblasts in animals with different levels of sensitivity to Leishmania infantum and Leishmania mexicana (Kinetoplastida: Trypanosomatidae)]. Rev Biol Trop. 2004;52: 261–7. Available: http://www.ncbi.nlm.nih.gov/pubmed/17357424

11. Rodríguez JH, Mozos E, Méndez A, Pérez J, Gómez-Villamandos JC. Leishmania Infection of Canine Skin Fibroblasts In Vivo. Vet Pathol. 1996;33: 469–473. doi:10.1177/030098589603300423

683 12. Schwartzman JD, Pearson RD. The interaction of Leishmania donovani
684 promastigotes and human fibroblasts in vitro. Am J Trop Med Hyg. 1985;34:
685 850–5. Available: http://www.ncbi.nlm.nih.gov/pubmed/4037177

686 13. Pace J, Hayman MJ, Galán JE. Signal transduction and invasion of epithelial
687 cells by S. typhimurium. Cell. 1993;72: 505–14. Available:
688 http://www.ncbi.nlm.nih.gov/pubmed/8382566

689 14. Valentin-Weigand P, Jungnitz H, Zock A, Rohde M, Chhatwal GS.
690 Characterization of group B streptococcal invasion in HEp-2 epithelial cells.
691 FEMS Microbiol Lett. 1997;147: 69–74. Available:
692 http://www.ncbi.nlm.nih.gov/pubmed/9037766

693 15. Dramsi S, Cossart P. Listeriolysin O-mediated calcium influx potentiates entry of
694 Listeria monocytogenes into the human Hep-2 epithelial cell line. Infect Immun.
695 2003;71: 3614–8. Available: http://www.ncbi.nlm.nih.gov/pubmed/12761148

696 16. Schettino PM, Majumder S, Kierszenbaum F. Regulatory effect of the level of
697 free Ca2+ of the host cell on the capacity of Trypanosoma cruzi to invade and
698 multiply intracellularly. J Parasitol. 1995;81: 597–602. Available:
699 http://www.ncbi.nlm.nih.gov/pubmed/7623203

700 17. Tardieux I, Nathanson MH, Andrews NW. Role in host cell invasion of
701 Trypanosoma cruzi-induced cytosolic-free Ca2+ transients. J Exp Med.
702 1994;179: 1017–22. Available: http://www.ncbi.nlm.nih.gov/pubmed/8113670

703 18. Reddy A, Caler E V, Andrews NW. Plasma membrane repair is mediated by
704 Ca(2+)-regulated exocytosis of lysosomes. Cell. 2001;106: 157–69. Available:
705 http://www.ncbi.nlm.nih.gov/pubmed/11511344

706 19. Tam C, Idone V, Devlin C, Fernandes MC, Flannery A, He X, et al. Exocytosis
707 of acid sphingomyelinase by wounded cells promotes endocytosis and plasma
708 membrane repair. J Cell Biol. 2010;189: 1027–1038. doi:10.1083/jcb.201003053

709 20. Idone V, Tam C, Goss JW, Toomre D, Pypaert M, Andrews NW. Repair of
710 injured plasma membrane by rapid Ca $^{2+}$ -dependent endocytosis. J Cell Biol.
711 2008;180: 905–914. doi:10.1083/jcb.200708010

712 21. Tardieux I, Webster P, Ravesloot J, Boron W, Lunn JA, Heuser JE, et al.
713 Lysosome recruitment and fusion are early events required for trypanosome
714 invasion of mammalian cells. Cell. Cell Press; 1992;71: 1117–1130.
715 doi:10.1016/S0092-8674(05)80061-3

716 22. Encarnação M, Espada L, Escrevente C, Mateus D, Ramalho J, Michelet X, et al.
717 A Rab3a-dependent complex essential for lysosome positioning and plasma
718 membrane repair. J Cell Biol. The Rockefeller University Press; 2016;213: 631–
719 40. doi:10.1083/jcb.201511093

720 23. Hissa B, Pontes B, Roma PMS, Alves AP, Rocha CD, Valverde TM, et al.
721 Membrane cholesterol removal changes mechanical properties of cells and
722 induces secretion of a specific pool of lysosomes. PLoS One. Public Library of
723 Science; 2013;8: e82988. doi:10.1371/journal.pone.0082988

724 24. Collot M, Louvard D, Singer SJ. Lysosomes are associated with microtubules
725 and not with intermediate filaments in cultured fibroblasts. Proc Natl Acad Sci U
726 S A. National Academy of Sciences; 1984;81: 788–92. Available:
727 http://www.ncbi.nlm.nih.gov/pubmed/6366790

728 25. Couto NF, Pedersane D, Rezende L, Dias PP, Corbani TL, Bentini LC, et al.

LAMP-2 absence interferes with plasma membrane repair and decreases T. cruzi host cell invasion. PLoS Negl Trop Dis. 2017;11. doi:10.1371/journal.pntd.0005657

26. Holbrook TW, Palczuk NC. Leishmania in the chick embryo. IV. Effects of embryo age and hatching, and behavior of L. donovani in cultures of chick fibroblasts. Exp Parasitol. 1975;37: 398–404. Available: http://www.ncbi.nlm.nih.gov/pubmed/1126423

27. Rittig MG, Bogdan C. Leishmania-host-cell interaction: complexities and alternative views. Parasitol Today. 2000;16: 292–7. Available: http://www.ncbi.nlm.nih.gov/pubmed/10858648

28. Rodríguez A, Samoff E, Rioult MG, Chung A, Andrews NW. Host cell invasion by trypanosomes requires lysosomes and microtubule/kinesin-mediated transport. J Cell Biol. The Rockefeller University Press; 1996;134: 349–62. Available: http://www.ncbi.nlm.nih.gov/pubmed/8707821

29. Andrews NW, Corrotte M, Castro-Gomes T. Above the fray: Surface remodeling by secreted lysosomal enzymes leads to endocytosis-mediated plasma membrane repair. Semin Cell Dev Biol. 2015;45: 10–17. doi:10.1016/j.semcdb.2015.09.022

30. Forestier C-L, Machu C, Loussert C, Pescher P, Späth GF. Imaging host cell-Leishmania interaction dynamics implicates parasite motility, lysosome recruitment, and host cell wounding in the infection process. Cell Host Microbe. 2011;9: 319–30. doi:10.1016/j.chom.2011.03.011

31. Noronha FS, Cruz JS, Beirão PS, Horta MF. Macrophage damage by Leishmania amazonensis cytolysin: evidence of pore formation on cell membrane. Infect

Immun. 2000;68: 4578–84. Available: http://www.ncbi.nlm.nih.gov/pubmed/10899858

32. Castro-Gomes T, Almeida-Campos FR, Calzavara-Silva CE, da Silva RA, Frézard F, Horta MF. Membrane binding requirements for the cytolytic activity of *Leishmania amazonensis* leishporin. FEBS Lett. 2009;583: 3209–3214. doi:10.1016/j.febslet.2009.09.005

33. Bennett CL, Misslitz A, Colledge L, Aebischer T, Blackburn CC. Silent infection of bone marrow-derived dendritic cells by Leishmania mexicana amastigotes. Eur J Immunol. 2001;31: 876–83. doi:10.1002/1521-4141(200103)31:3<876::AID-IMMU876>3.0.CO;2-I

34. Smith RS, Smith TJ, Blieden TM, Phipps RP. Fibroblasts as sentinel cells. Synthesis of chemokines and regulation of inflammation. Am J Pathol. 1997;151: 317–22. Available: http://www.ncbi.nlm.nih.gov/pubmed/9250144

35. Shaw TJ, Martin P. Wound repair: a showcase for cell plasticity and migration. Curr Opin Cell Biol. 2016;42: 29–37. doi:10.1016/j.ceb.2016.04.001

36. Real F, Florentino PTV, Reis LC, Ramos-Sanchez EM, Veras PST, Goto H, et al. Cell-to-cell transfer of *L eishmania amazonensis* amastigotes is mediated by immunomodulatory LAMP-rich parasitophorous extrusions. Cell Microbiol. 2014;16: 1549–1564. doi:10.1111/cmi.12311

37. Carneiro MBH, Roma EH, Ranson AJ, Doria NA, Debrabant A, Sacks DL, et al. NOX2-Derived Reactive Oxygen Species Control Inflammation during *Leishmania amazonensis* Infection by Mediating Infection-Induced Neutrophil Apoptosis. J Immunol. 2018;200: 196–208. doi:10.4049/jimmunol.1700899

775 38. Späth GF, Beverley SM. A Lipophosphoglycan-Independent Method for
776 Isolation of Infective Leishmania Metacyclic Promastigotes by Density Gradient
777 Centrifugation. Exp Parasitol. Academic Press; 2001;99: 97–103.
778 doi:10.1006/EXPR.2001.4656

779 39. Luo J, Zhu Y, Zhu MX, Hu H. Cell-based calcium assay for medium to high
780 throughput screening of TRP channel functions using FlexStation 3. J Vis Exp.
781 MyJoVE Corporation; 2011; doi:10.3791/3149

782 40. Rodríguez A, Webster P, Ortego J, Andrews NW. Lysosomes Behave as Ca 2 2 -
783 regulated Exocytic Vesicles in Fibroblasts and Epithelial Cells. J Cell Biol.
784 1997;137: 93–104. Available:
785 https://www.ncbi.nlm.nih.gov/pmc/articles/PMC2139854/pdf/18982.pdf

786 **LEGEND TO FIGURES**

787 **Fig 1 – Invasion of MEFs by *L. amazonensis in vitro* depends on parasite viability**
788 **and infectivity and does not require host cell actin polymerization.** (A) MEF infected
789 by *L. amazonensis*. 3D reconstruction assembled from all z-stacks obtained of an infected
790 MEF displaying both sides of the infected cell. MEFs were incubated with *LLa*-RFP for
791 2 h at 37°C, labeled to visualize F-actin (green) and nuclei (blue) and imaged. (B) Single
792 focal plane of the same infected fibroblast (Fig. 1A) shows the parasite (red) not co-
793 localized with host cell F-actin (green). (C) Time course of MEF infection by *L.*
794 *amazonensis*. Infection was performed as described in 1A, at the indicated time points
795 cells were collected and infection quantified by FACS. Non-infected cells (NI) were gated
796 as negative controls. (D) *L. amazonensis* infection of MEFs pre-treated with cytochalasin-
797 D (CD). MEFs were pre-treated (green) or not (red) with 10 μM CD for 15 min, infected
798 with *LLa*-RFP for 4 h and infection was quantified by FACS. (E) MEF infection by

799 procyclic or metacyclic promastigotes. MEFs were infected with *LLa*-RFP metacyclic
800 (red) or procyclic (orange) promastigotes. Infection was performed and quantified as
801 indicated in 1D. (F and G) MEF infection with live, PFA-fixed and heat-killed *LLa*-RFP.
802 MEFs were incubated with live (red), heat-treated (green) or PFA-fixed (orange) *LLa*-
803 RFP for 4 (F) or 24 h (G) and infection was quantified by FACS. (H) Infected MEF with
804 host cell lysosomal staining. Cells were labeled by immunofluorescence to visualize
805 lysosomes (green), nuclei (blue) and imaged using Axio Imager ApoTome2 Microscope
806 (Zeiss) to obtain a single focal plane of a MEF infected with *LLa*-RFP (red) after 2 h of
807 infection.

808 **Fig 2 – *L. amazonensis* resides in tight individual vacuoles rich in lysosomal markers**
809 **and remains viable after differentiation into intracellular stages.** (A) *L. amazonensis*
810 replicates inside MEFs. After infection by *LLa*-RFP, the cell population was analyzed by
811 FACS at 4 and 24 h post infection. The mean fluorescence intensity (MFI) of the infected
812 population was calculated and is indicated for each curve. (B and C) *L. amazonensis*
813 amastigotes residing in perinuclear vacuoles co-localized with lysosomal markers. MEFs
814 were incubated with *LLa*-RFP for 24 h at 37°C and then labeled to visualize lysosomes
815 (green) and nuclei (blue) and imaged using BX60 Upright Compound Fluorescence
816 Microscope (Olympus). The image shows each channel individually and also merged
817 with (B) or without the bright field (C). (D to G) Transmission electron microscopy
818 analysis of MEFs infected with *L. amazonensis*. Cells were infected and prepared for
819 electron microscopy after 4 h (D) or 7 days after infection (F). Asterisks show parasites
820 inside MEFs. (E and G) Zoom-ins from the region indicated by a black asterisk in D and
821 F, respectively. Insert in E shows a detail of the parasite PM with its typical subpellicular
822 microtubules (SM) juxtaposed with the parasitophorous vacuole membrane (PVM). In G
823 an amastigote is shown within the parasitophorous vacuole (PV) with the flagellar pocket

824 (FP), nuclei (N) and mitochondrion (M). (H and I) Hematoxylin-eosin staining of MEFs
825 10 days after infection. (J) Promastigotes obtained from MEF-derived amastigotes.
826 Infected MEFs shown in H and I were scraped, inoculated into insect media and imaged
827 10 days later by conventional light microscopy.

828 **Fig 3 – Internalization of *L. amazonensis* in MEFs involves calcium influx, PM**
829 **permeabilization and intracellular calcium signaling.** (A) Visualization of calcium
830 fluxes induced by *L. amazonensis* in MEFs. MEFs were loaded with the calcium-sensitive
831 probe Fluo-4AM and incubated with *LLa*-RFP. Cells were imaged by live confocal
832 microscopy at 10 frames/s. (B) Graphical representation of intracellular calcium
833 transients obtained from individual analysis of the 9 indicated cells, from the experiment
834 in 3A. (C) Assessment of host cell PM permeability during *L. amazonensis* infection in
835 MEFs. A MEF monolayer was incubated with *L. amazonensis* in the presence of
836 propidium iodide (PI). After infection, the cells were examined by fluorescence
837 microscopy. (D) Quantification of cell permeability in MEFs during *L. amazonensis*
838 infection in the presence or absence of calcium. MEFs were incubated with *L.*
839 *amazonensis* in the presence or absence of calcium for 2 h. PI was added only at the end
840 of the experiment and the cell population was analyzed by FACS. (E) Extracellular
841 calcium favors infection. MEFs were incubated with *LLa*-RFP in increasing
842 concentrations of extracellular calcium for 4 h and infection was quantified by FACS. (F)
843 Detection of parasite-induced intracellular calcium transients in MEFs. MEFs were
844 loaded with the calcium probe Fluo-4AM and incubated with *LLa*-RFP in the absence of
845 extracellular calcium. Cells were imaged by live confocal microscopy at 10 frames/s. G)
846 Graphical representation of intracellular calcium transients obtained from individual
847 analysis of 7 indicated cells, from the experiment in 3F. The videos used to build figures
848 3A, B, F and G are provided as supplementary data.

Fig 4 – *L. amazonensis* induces lysosomal exocytosis during cell entry in MEFs. (A) Lysosomes are recruited to parasite binding site during *L. amazonensis* invasion. MEFs were incubated with *LLa*-RFP for 30 min, permeabilized and labeled to visualize lysosomes (green) and nuclei (blue), followed by fluorescence microscopy - white arrows indicate parasites interacting with the host cell (bright field) and attracting host cell lysosomes. (B) Same as A but cells were not permeabilized to visualize only the exposure of lysosomal luminal epitopes on the plasma membrane. (C) Quantification of lysosomal epitope exposure on the surface of MEFs incubated with live (blue) or PFA-fixed *L. amazonensis* (green) removed from the dish by scraping and analyzed by FACS. (D to E) Exocytosis of host cell lysosomal enzymes during *L. amazonensis* invasion in MEFs. (C) The activity of beta-Hex was assayed in supernatants of cells incubated with living (solid line) and PFA-fixed *L. amazonensis* (dashed line). Controls with *L. amazonensis* alone were carried out (dotted line). (E) Supernatants were analyzed by western blotting using anti-ASM or anti-cathepsin D (Cat-D) antibodies. (F) Endocytosis quantification in MEFs incubated with *LLa*-RFP. MEF PM was labeled with A-488-conjugated WGA before incubation with parasites for 15 min. After parasite removal the extracellular fluorescence was quenched by trypan blue and the endocytosed dye was quantified by FACS. (G to H) Detection of lysosomal markers, ceramide and LAMP recently formed *L. amazonensis* vacuoles. MEFs were infected with *LLa*-RFP for 1 h and labeled to visualize lysosomes (green) (G), ceramide (green) (H), DAPI (blue) to stain nuclei, and imaged by fluorescence microscopy.

Fig 5 – Lysosomes are recruited at early steps of *L. amazonensis* infection in MEFs and envelop parasites as they gradually transform into intracellular amastigotes. MEFs were incubated with *LLa*-RFP (red). At indicated time points, infection was stopped, cells were fixed, labeled to visualize lysosomes (green) and nuclei (blue) and

874 imaged using BX60 Upright Compound Fluorescence Microscope (Olympus). Each
875 figure shows the three merged channels. (A) Lysosomal recruitment to infection sites.
876 The white arrow indicates the flagellar region and the red arrow the parasite body. (B) A
877 partially internalized parasite with the flagella totally surrounded by the lysosomal marker
878 LAMP-1. (C) Completely internalized parasite located at the perinuclear region
879 displaying flagellar shortening. (D) Internalized parasite presenting an ovoid form. (E)
880 Typical amastigote forms within LAMP-1-rich individual vacuoles at the perinuclear
881 region.

882 **Fig 6 – Host cell lysosome positioning and lysosomal content are crucial for MEF**
883 **invasion by *L. amazonensis*.** (A) Role of host cell microtubules in the invasion of MEFs
884 by *L. amazonensis*. MEFs were pre-treated with 20 μM nocodazole for 20 min, after drug
885 removal cells were incubated with *LLa*-RFP for 4 h at 37°C and infection was quantified
886 by FACS. (B to C) Cytochalasin-D and brefeldin-A treatment potentiates cell invasion in
887 a microtubule-dependent manner. (B) MEFs were treated (orange) or not (green) with 20
888 μM nocodazole for 20 min prior to treatment with 10 μM cytochalasin-D for 15 min.
889 After drug removal infection was performed as described above and quantified by FACS.
890 Infection of untreated MEFs by *LLa*-RFP is shown in red. (C) MEFs were treated (orange)
891 or not (green) with 20 μM nocodazole for 20 min prior to treatment with 10 μM brefeldin-
892 A for 30 min. After drug removal infection was performed as described above and
893 quantified by FACS. Infection of untreated MEFs by *LLa*-RFP is shown in red. (D, E
894 and F) Multi-infected cells visualized after cytochalasin-D and brefeldin-A treatments.
895 (D) Non-treated cells, (E) cytochalasin-D pre-treated cells and (F) brefeldin-A pre-treated
896 cells were infected as described above, fixed, labeled to visualize lysosomes (green) and
897 nuclei (blue) and imaged using BX60 Upright Compound Fluorescence Microscope
898 (Olympus). White arrows show internalized parasites. (G to I) Invasion of LAMP-2 and

LAMP-1/2 knockout MEFs by *L. amazonensis*. (G) WT (H) LAMP-2 knockout and (I) LAMP-1/2 double knockout MEFs were infected by *LLa*-RFP as described above and infection was quantified by FACS.

Fig 7 – Transient PM permeabilization enhances MEF invasion by *L. amazonensis*. (A) MEFs undergo PM repair in the presence of calcium. MEFs were incubated with increasing concentrations of the pore forming protein streptolysin-O (SLO) at 37°C for 15 min in the presence or absence of calcium. After the addition of PI the cell population was analyzed by FACS. The percentages of cell wounding (red) and cells that underwent PM repair (blue) are indicated in each graph. PM repair is indicated as the percentage of cells that excluded PI after being wounded by SLO. (B) Effect of SLO-triggered PM permeabilization in the invasion of MEFs by *L. amazonensis*. MEFs were incubated with *LLa*-RFP for 4 h. At 15 min of infection SLO was inoculated in the media at the indicated concentrations and infection was quantified by FACS. Infection of non-treated (red) and SLO-treated cells (green) is shown. The percentage of infection is indicated for each curve. (C to E) MEFs multi-infected by *L. amazonensis* after SLO-treatment. The experiment showed in 7B was carried out using 50 ng/mL SLO and cells were labeled to visualize lysosomes (green) and nuclei (blue) after 4 (C and D) or 24 h (E) of infection, and imaged using BX60 Upright Compound Fluorescence Microscope (Olympus). White arrows show internalized parasites.

Supplementary Fig S1 – (A and B) Series of optical sections of MEFs infected by *L. amazonensis* shown in Fig 1.A-B and Fig 1H. MEFs were incubated with *LLa*-RFP for 2 h at 37°C, labeled to visualize (A) F-actin (green) or (B) lysosomes (green) and nuclei (blue). Cells were imaged by Axio Imager ApoTome2 Microscope (Zeiss) to obtain confocal images. Z-stacks were obtained using structured illumination microscopy technology (SIM).

924 **Supplementary Fig S2 – Recently internalized parasites do not co-localize with F-**
925 **actin, attracts lysosomes to infection site and are covered by lysosomal proteins as**
926 **they enter cells.** MEFs were incubated with *LLa*-RFP (red). At indicated time points,
927 infection was stopped, cells were fixed, labeled to visualize lysosomes (green) and nuclei
928 (blue) and imaged using BX60 Upright Compound Fluorescence Microscope (Olympus).
929 Each figure shows the three merged channels. (A) Three different fields showing cells
930 containing recently internalized parasites (white arrows) and without actin coating. (B)
931 Lysosomes are recruited to infection site and enwrap parasites during cell invasion.
932 Parasites normally undergo transformation into amastigote forms.

933 **Supplementary Video 1 –** To visualize calcium fluxes induced by *L. amazonensis* MEFs
934 were loaded with the calcium probe Fluo-4AM and incubated with *LLa*-RFP in the
935 presence of 2 mM $CaCl_2$. Cells were imaged for 15 min in a Nikon C2 confocal
936 microscope at 10 frames/s.

937 **Supplementary Video 2 –** To visualize calcium transients generated intracellularly by *L.*
938 *amazonensis* MEFs were loaded with the calcium probe Fluo-4AM and incubated with
939 *LLa*-RFP in calcium-free medium. Cells were imaged for 15 min in a Nikon C2 confocal
940 microscope at 10 frames/s.

FIGURE 1

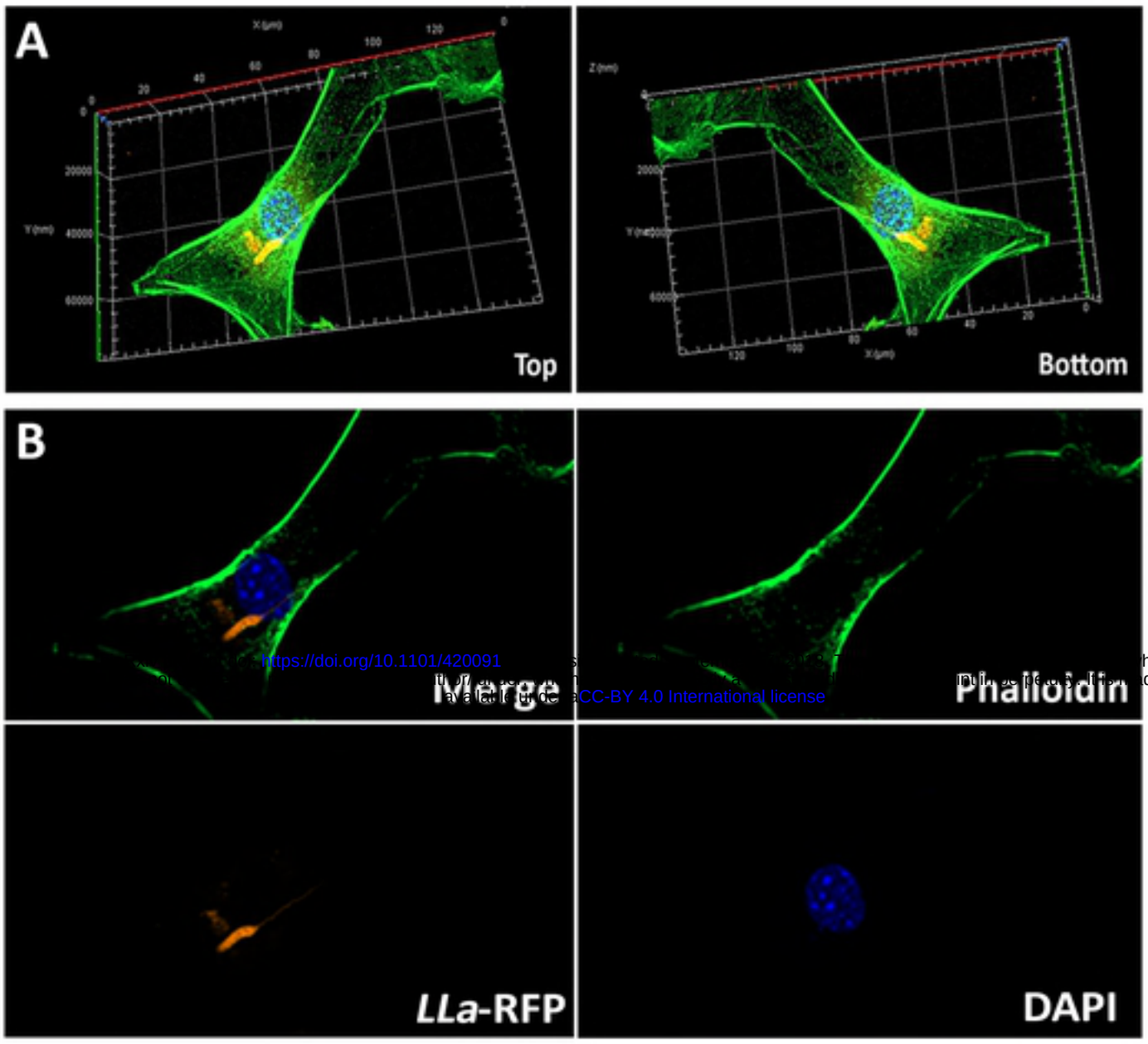

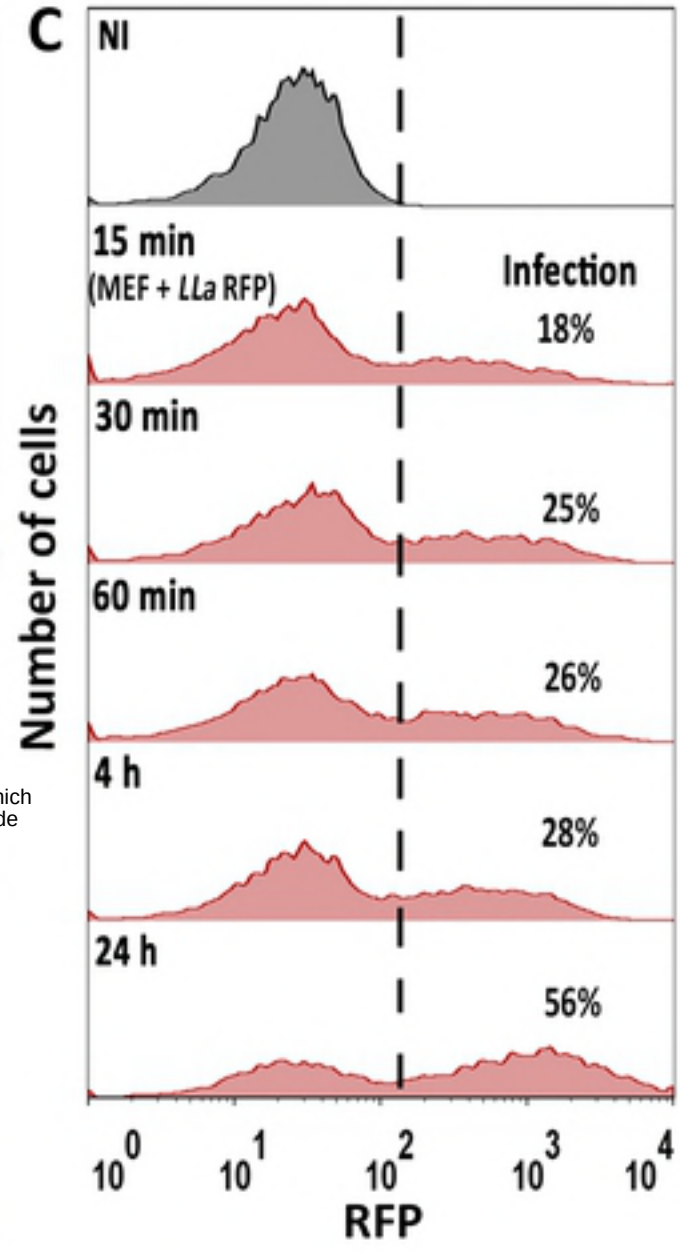

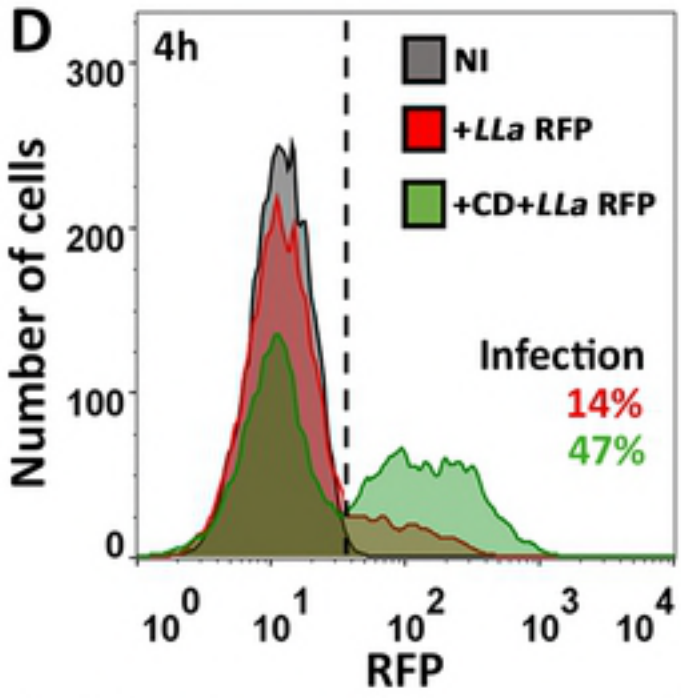

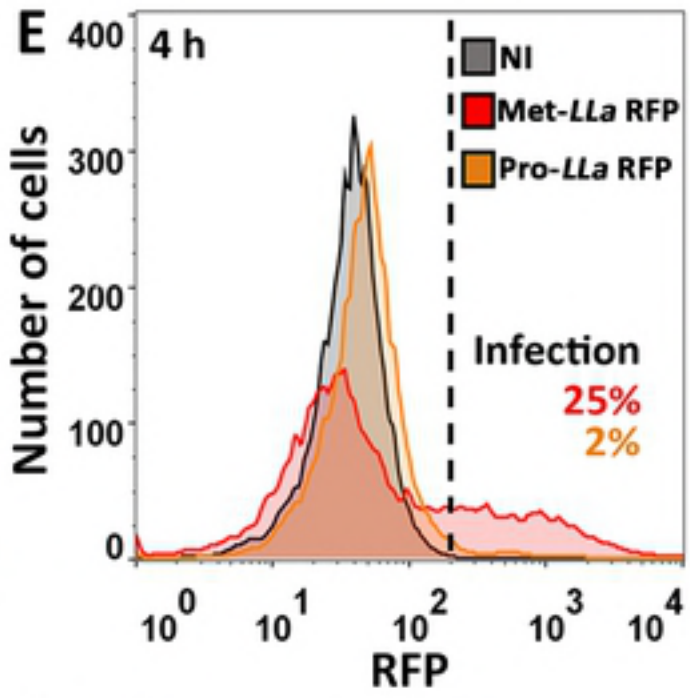

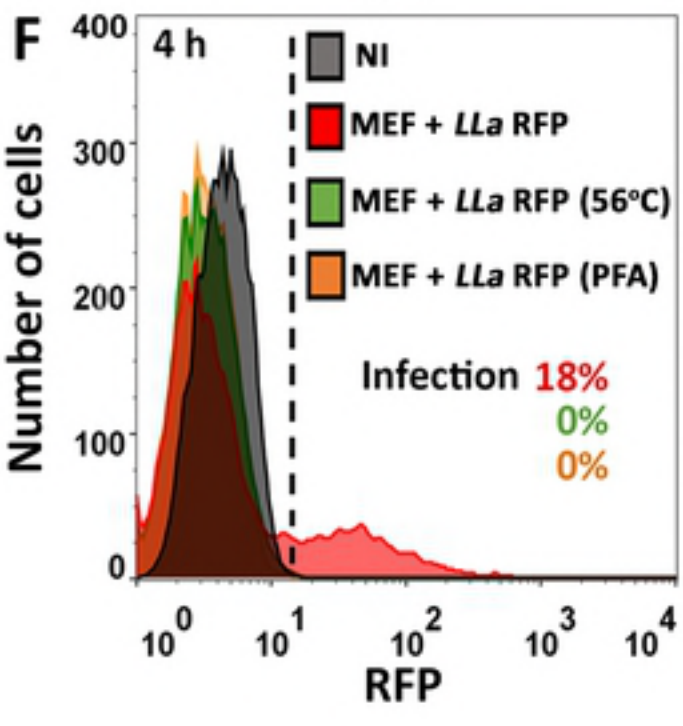

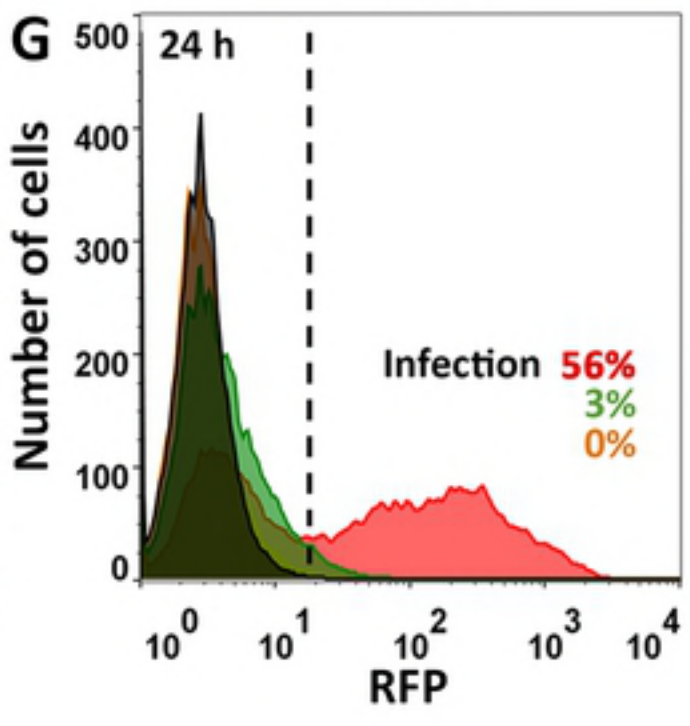

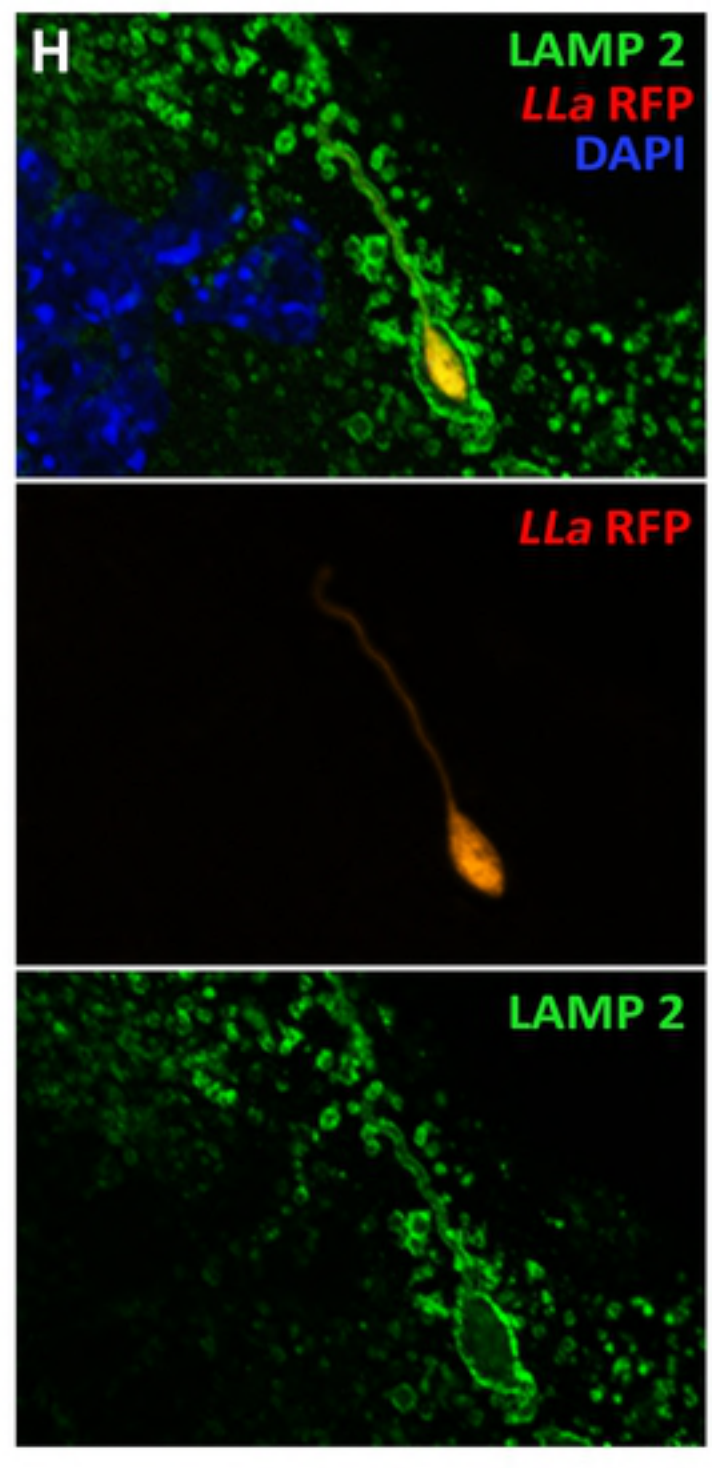

FIGURE 2

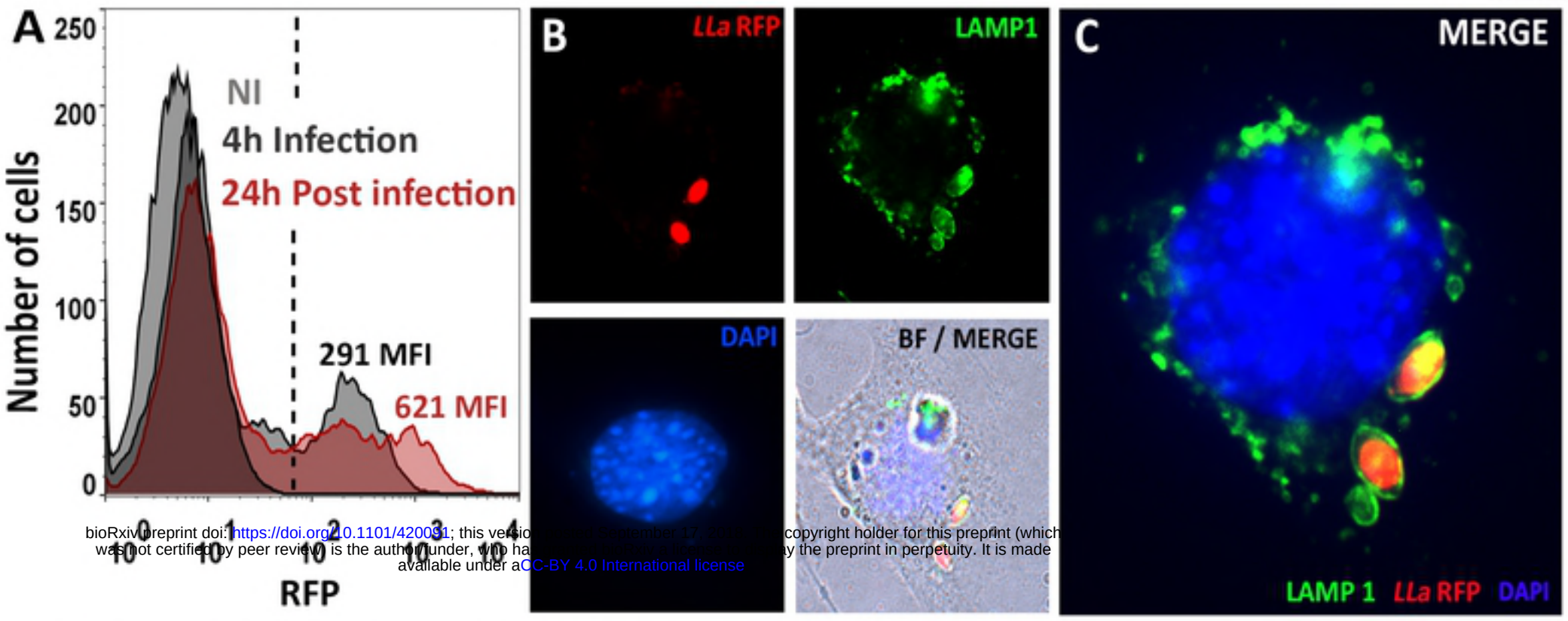

FIGURE 3

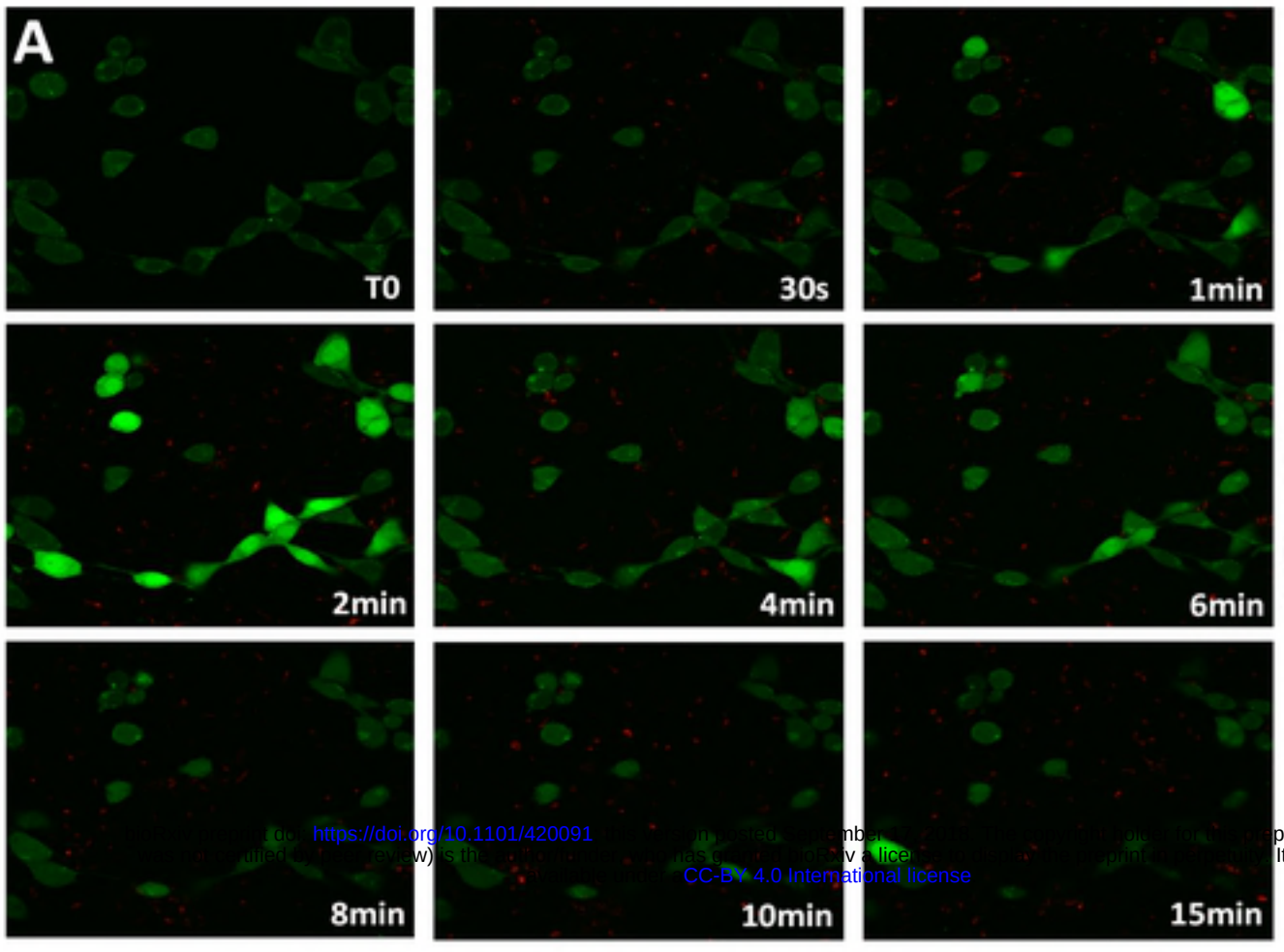

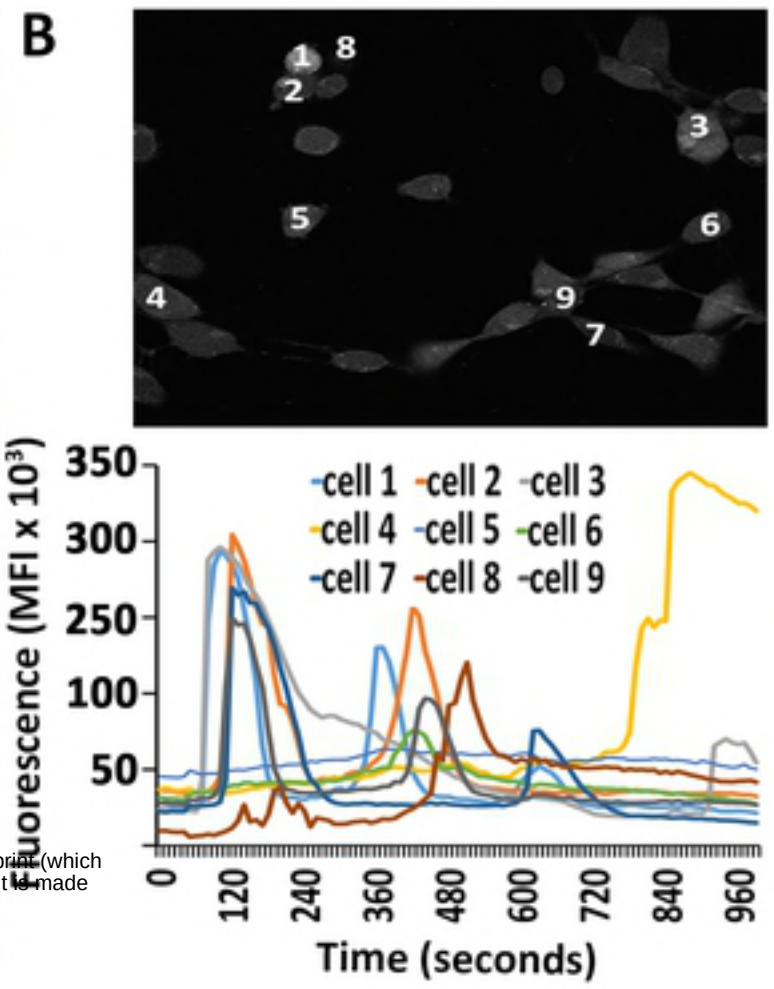

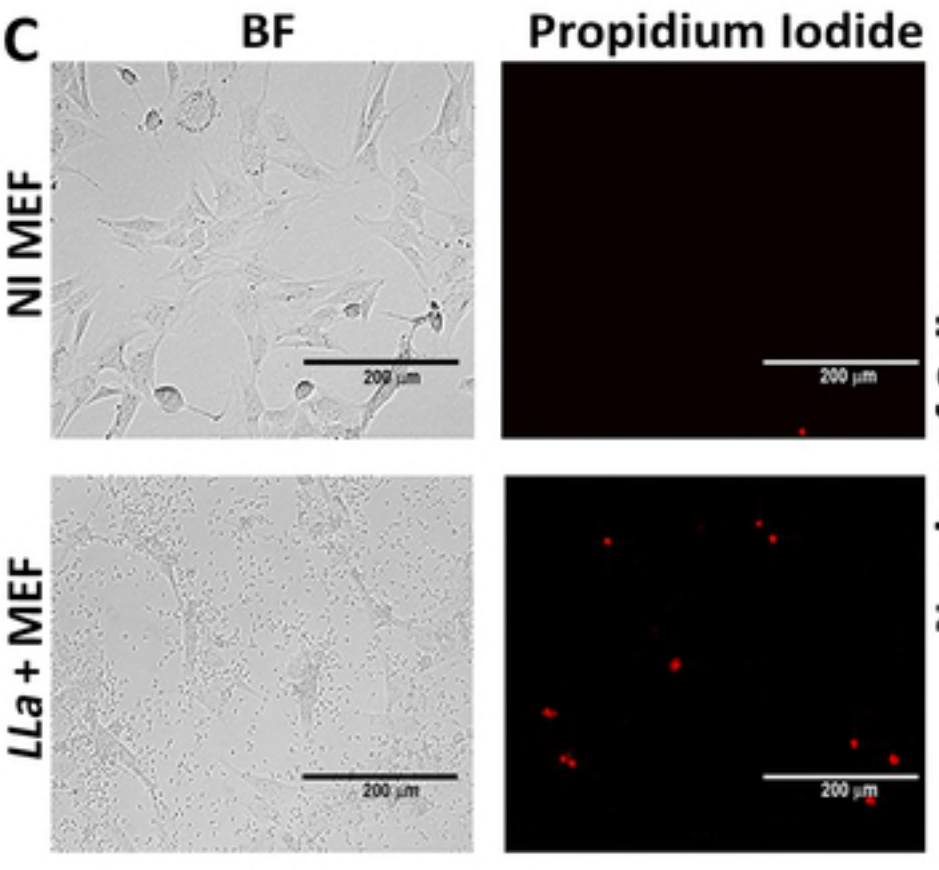

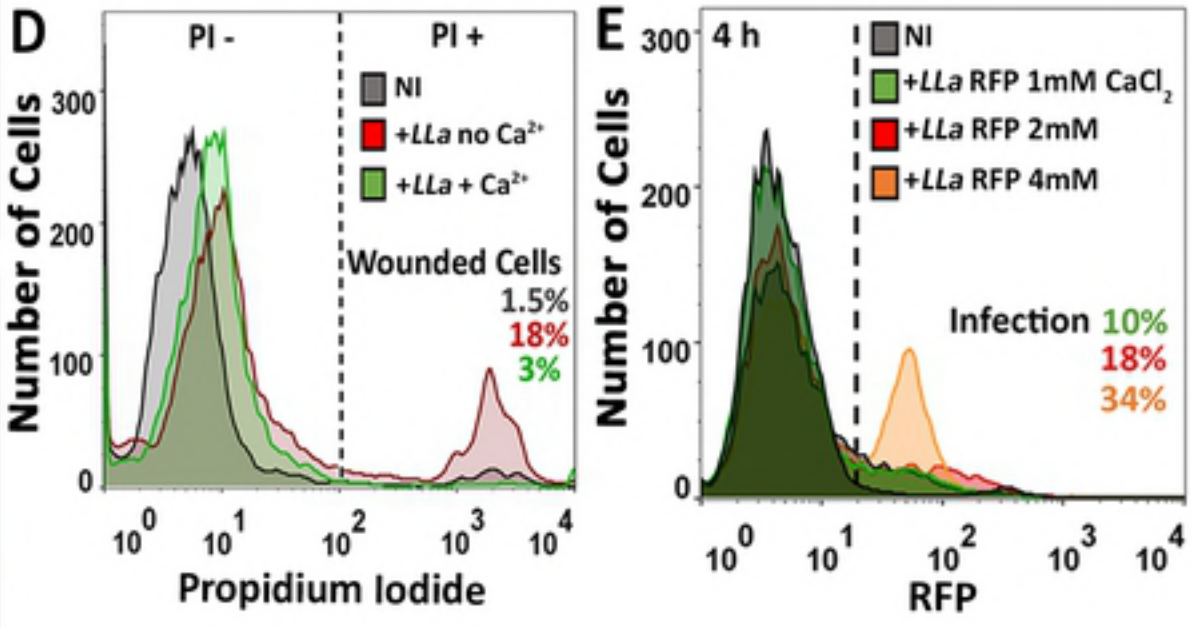

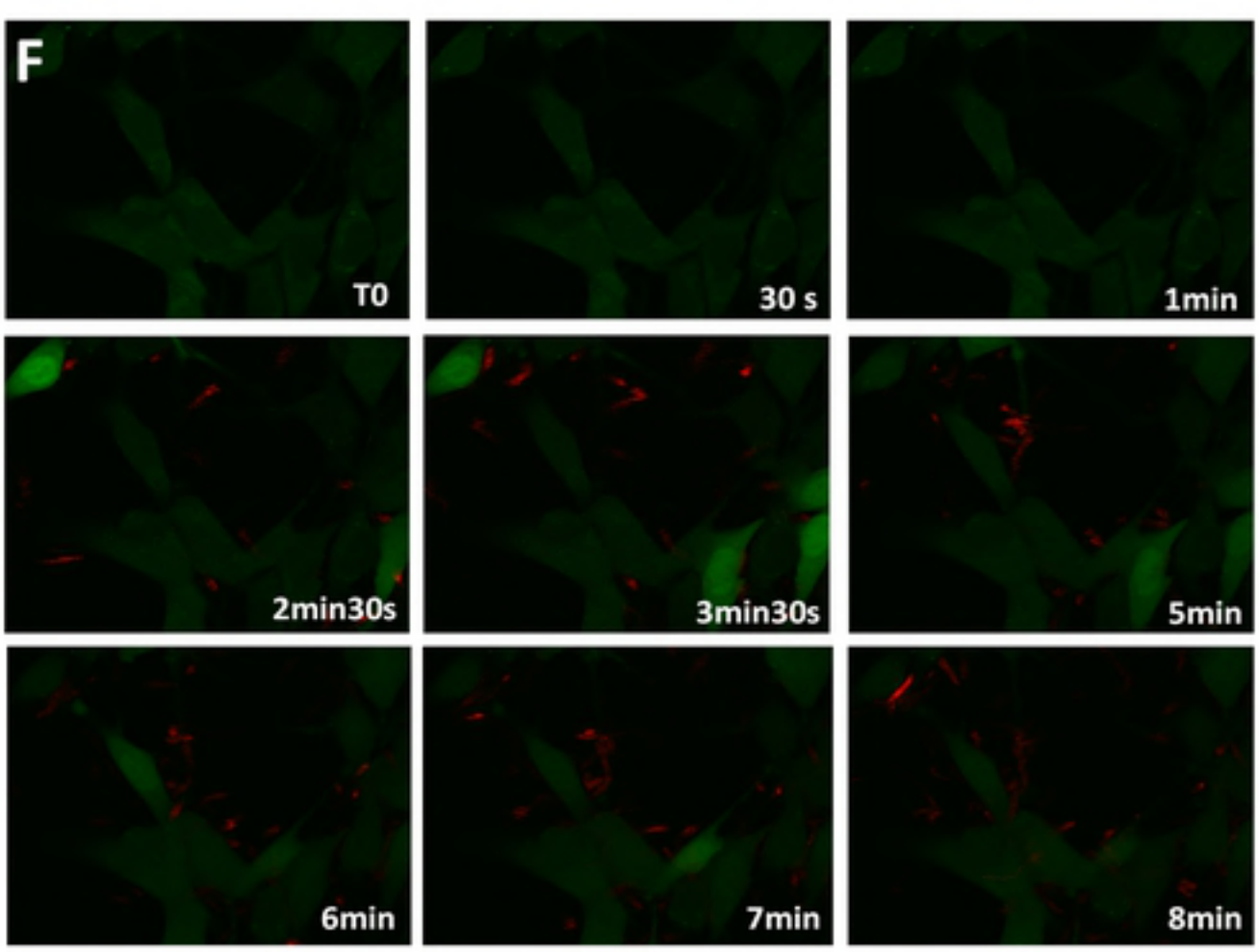

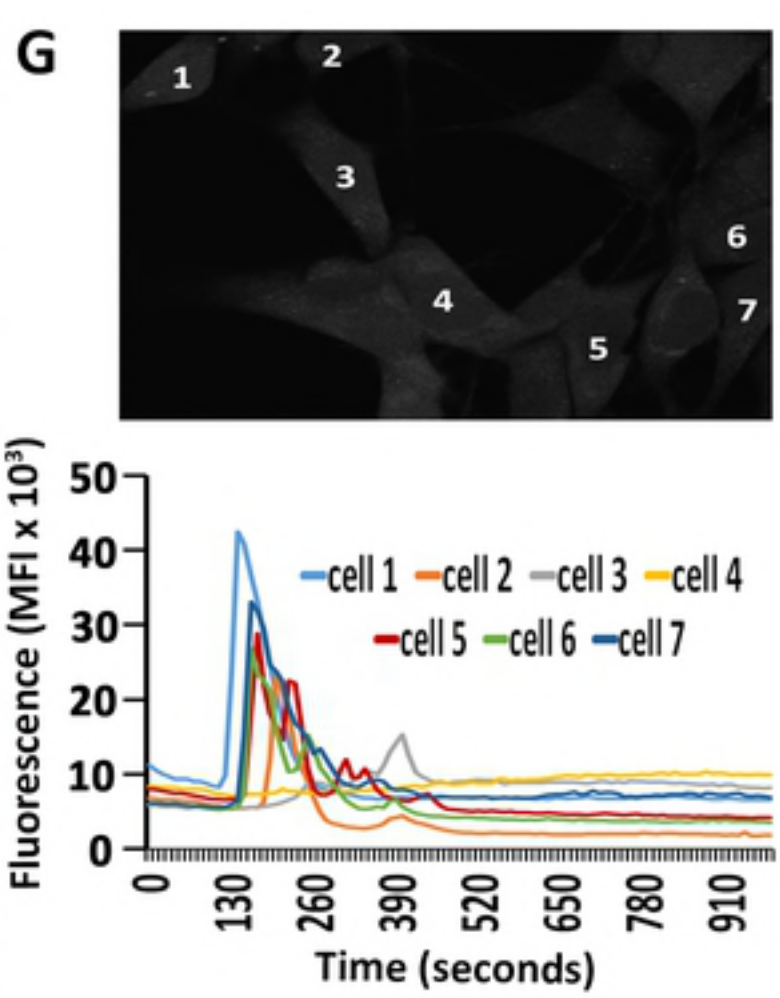

FIGURE 4

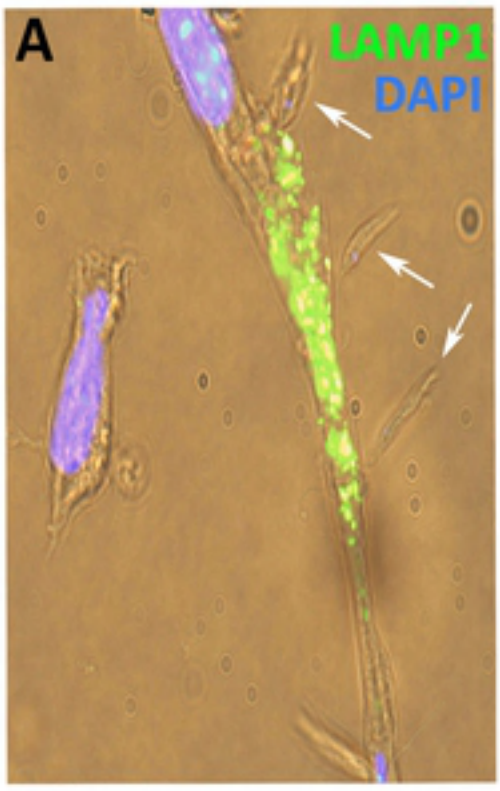

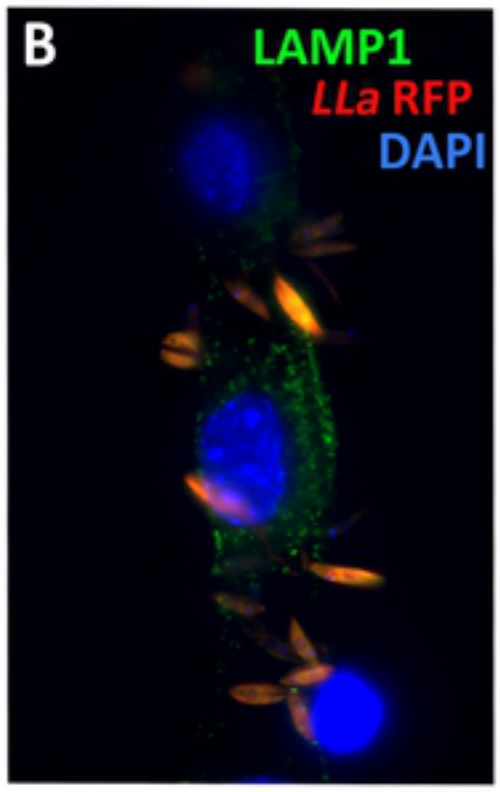

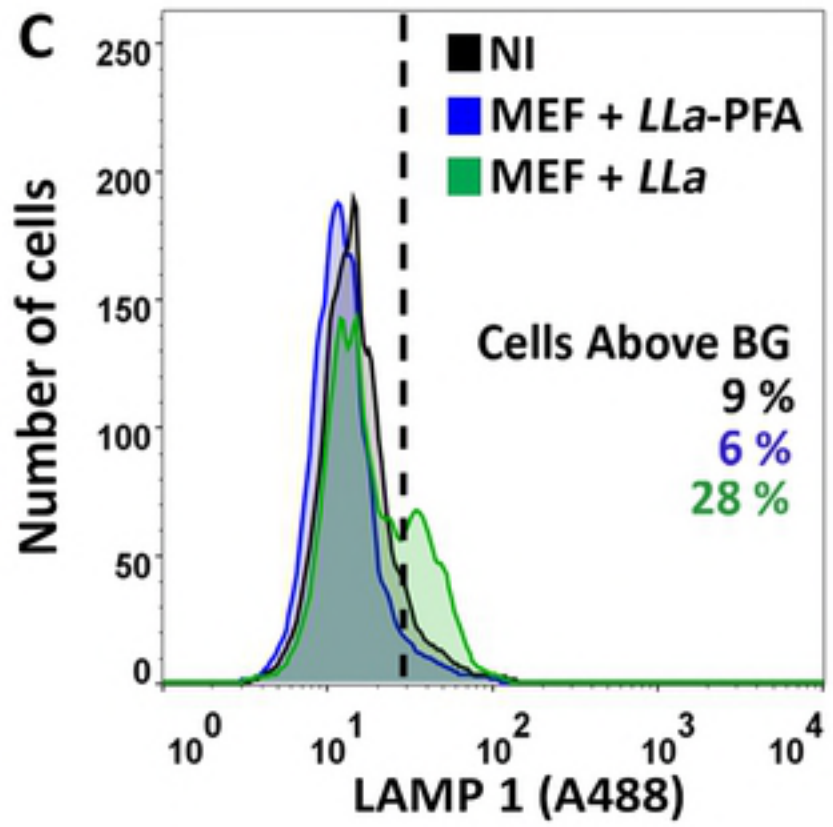

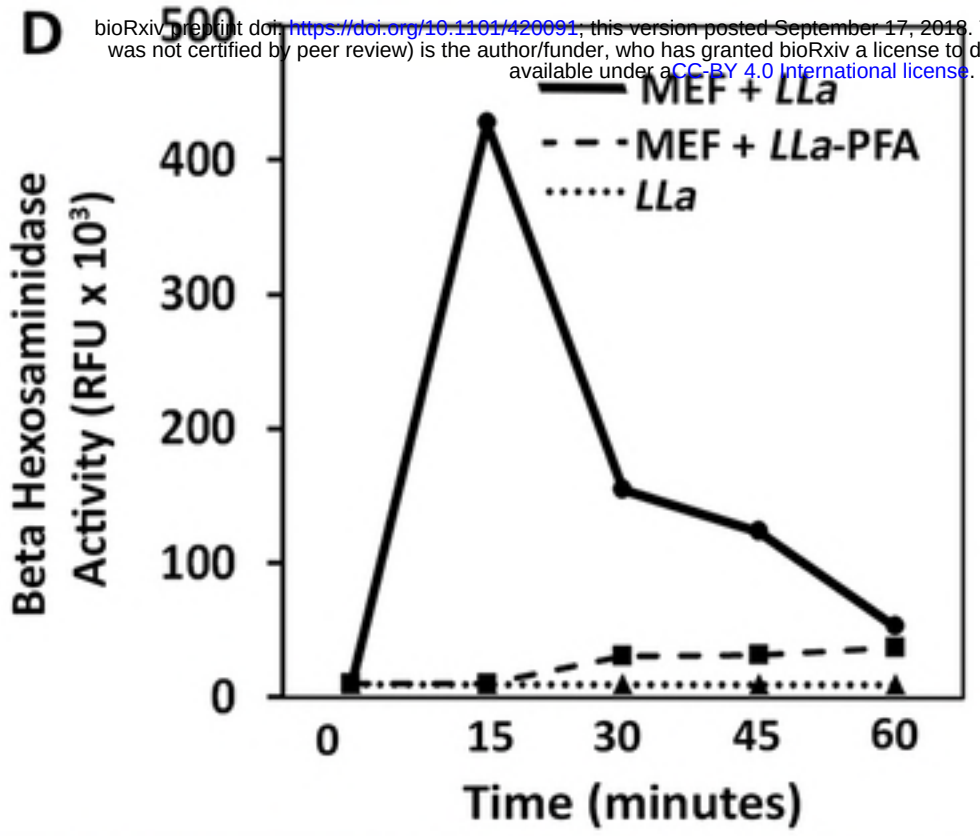

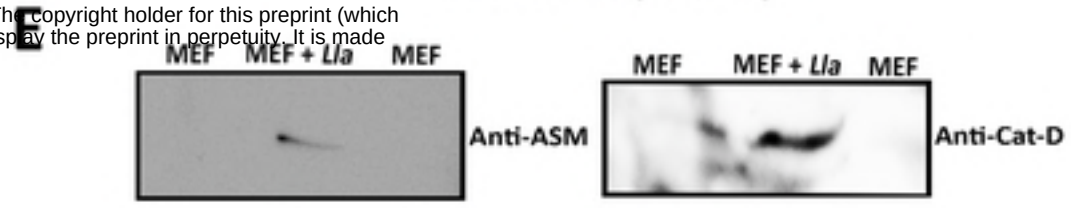

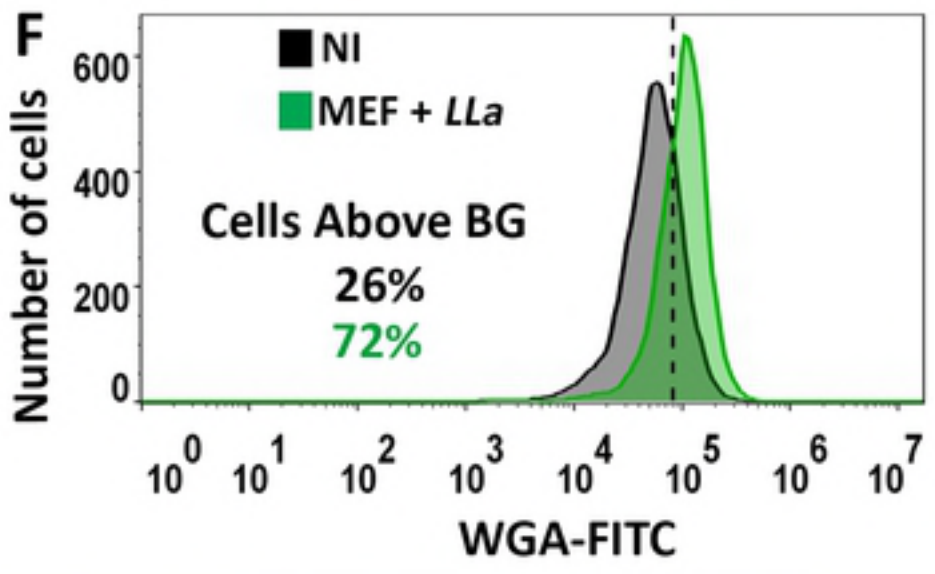

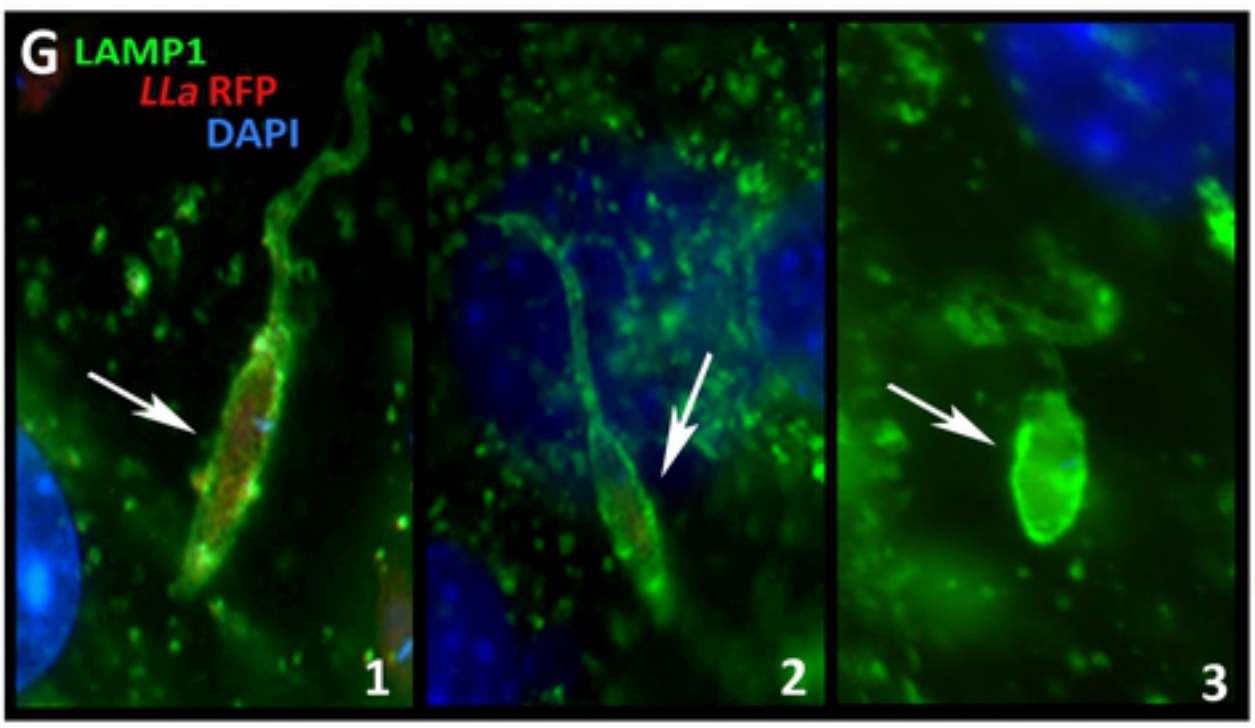

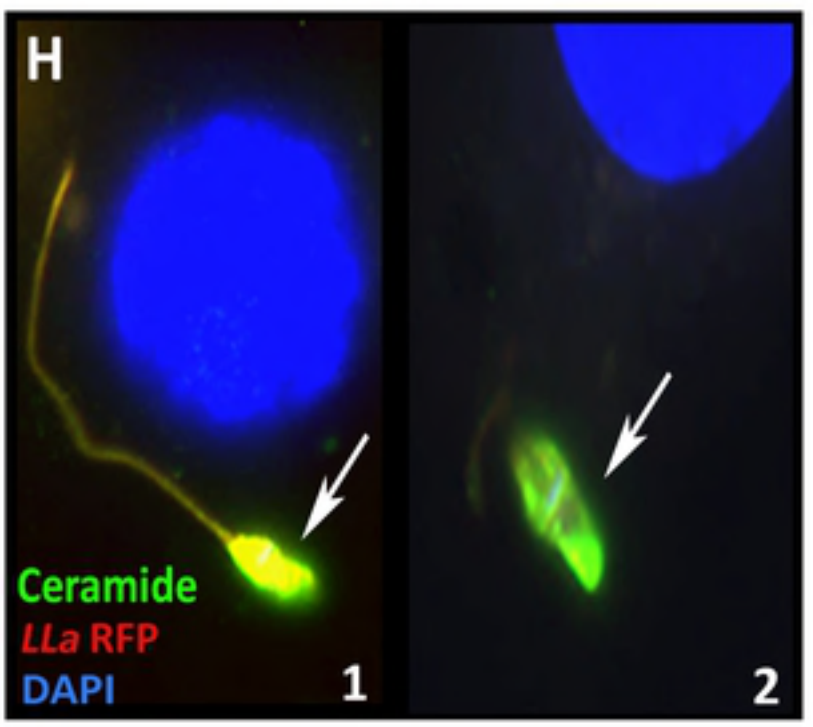

FIGURE 5

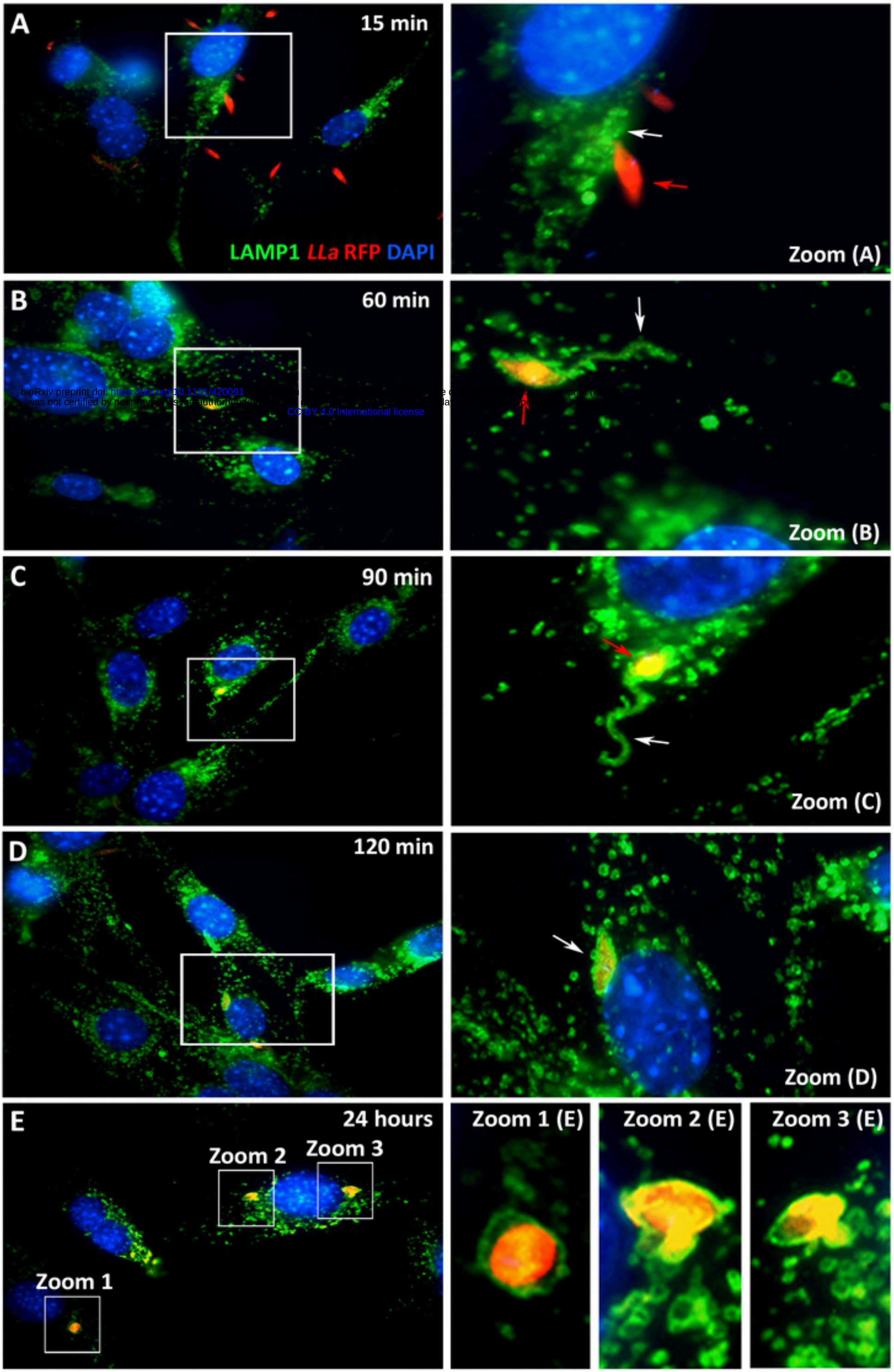

FIGURE 6

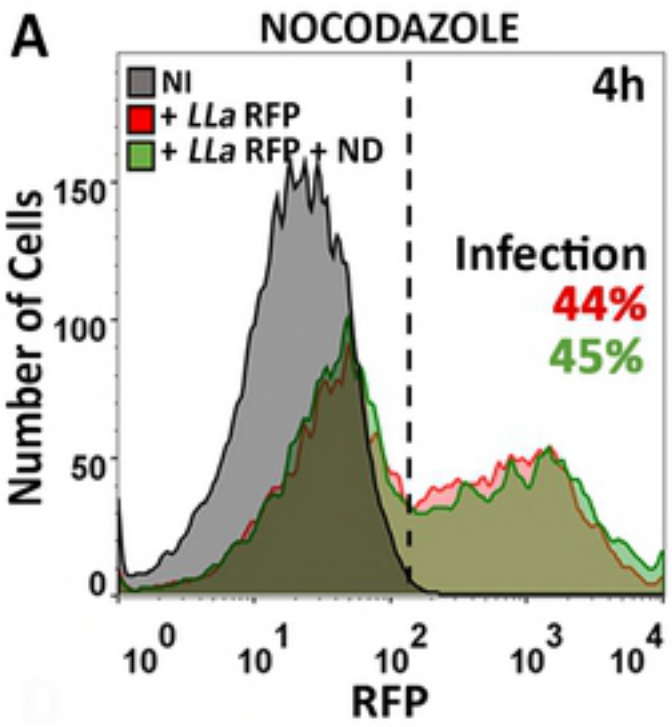

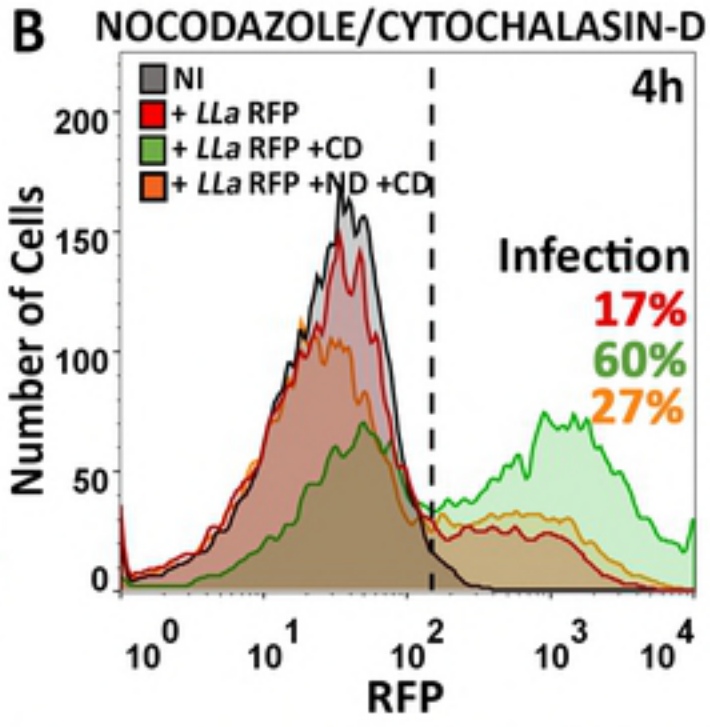

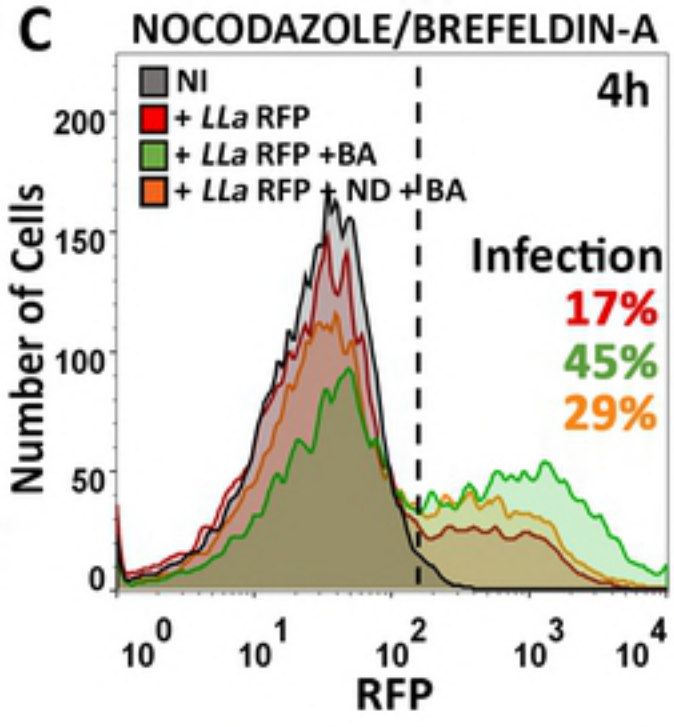

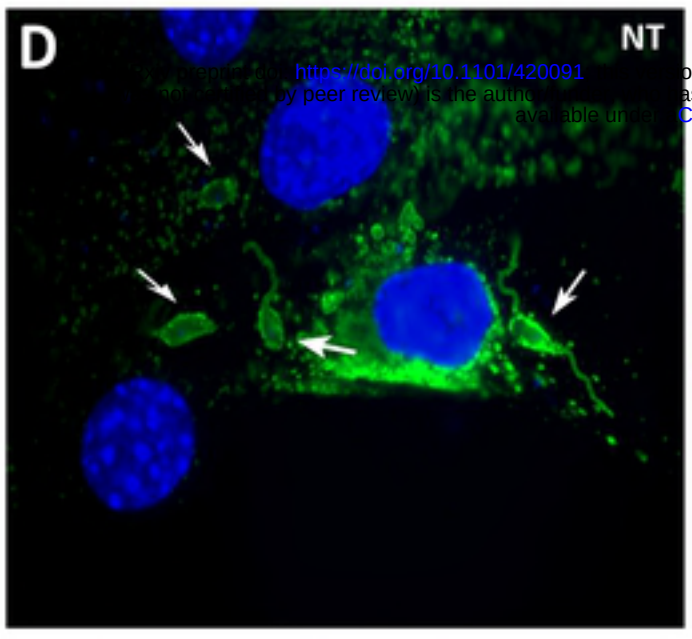

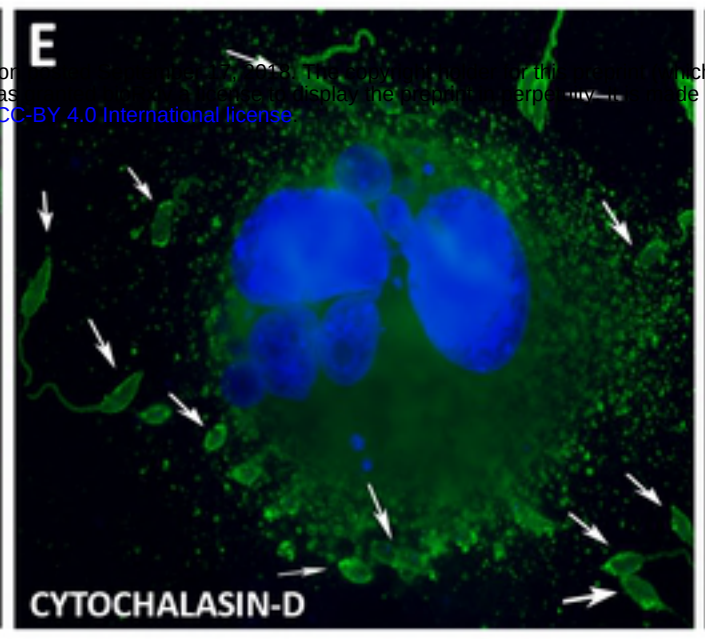

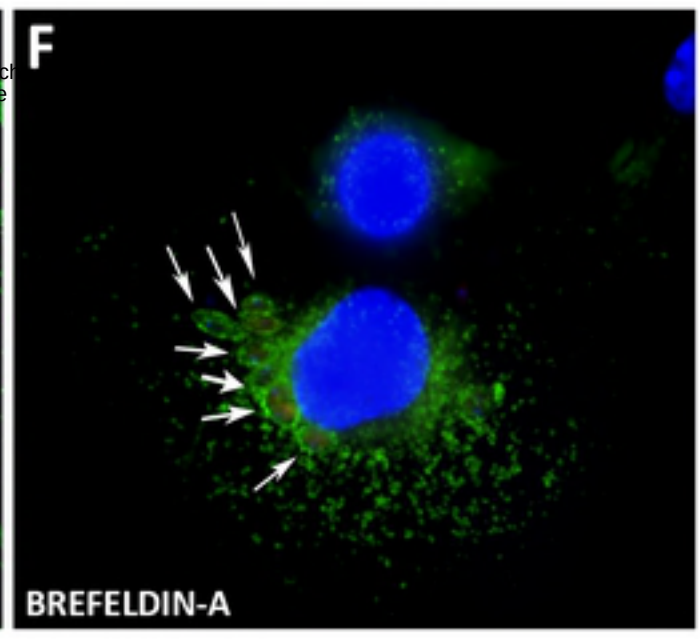

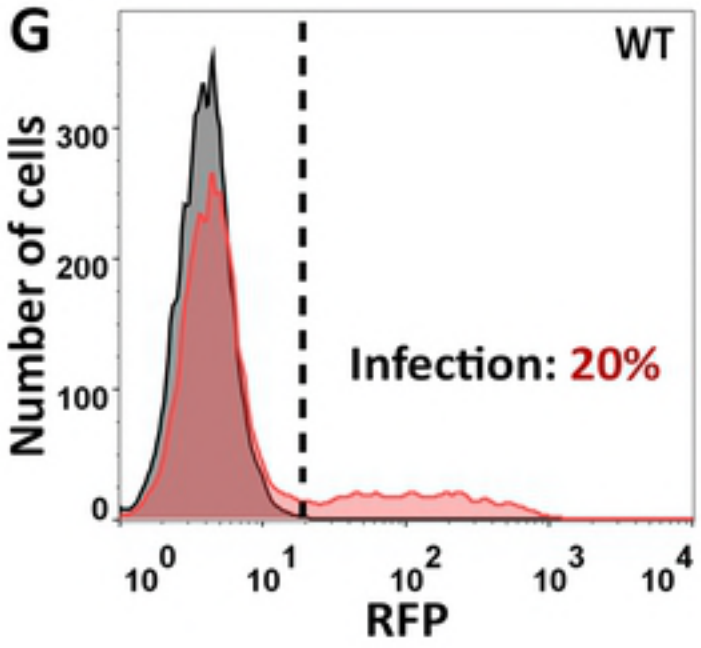

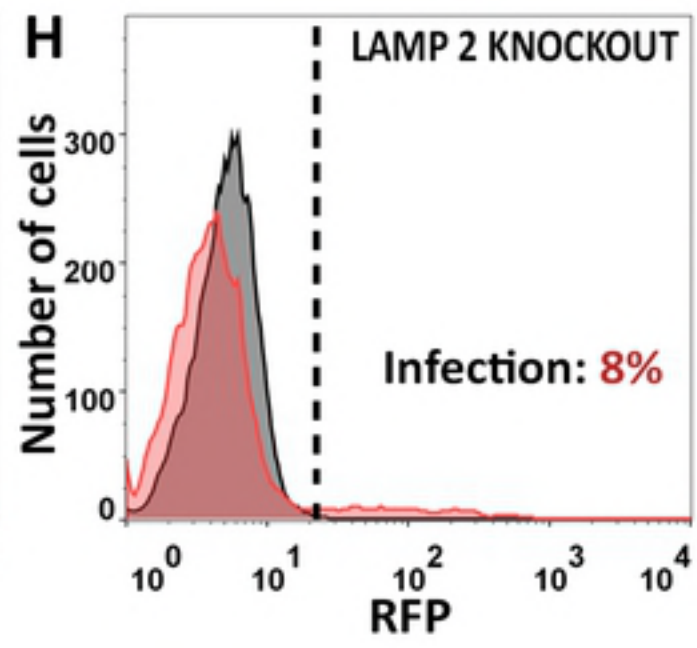

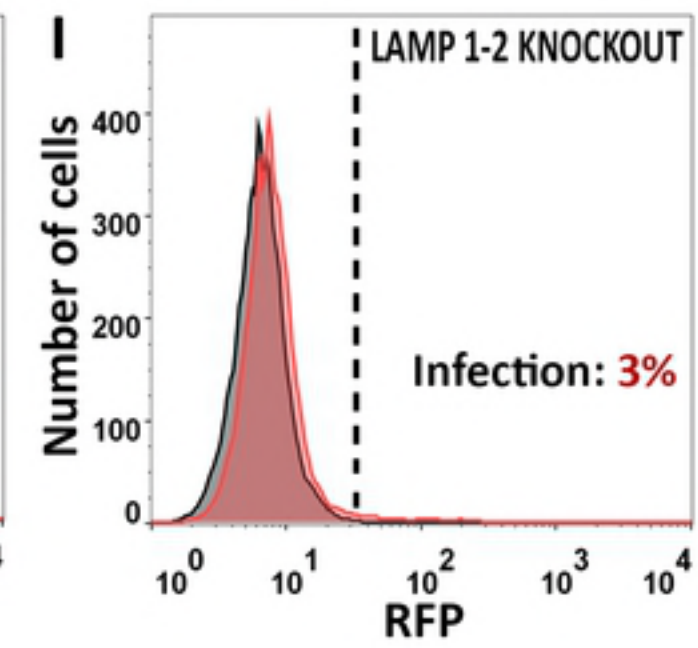

FIGURE 7